ANESTHESIOLOGY

Nerve Injury Triggers Time-dependent Activation of the Locus Coeruleus, Influencing Spontaneous Pain-like Behavior in Rats

Irene Suárez-Pereira, Ph.D., Carolina López-Martín, M.Sc., Carmen Camarena-Delgado, Ph.D., Meritxell Llorca-Torralba, Ph.D., Francisco González-Saiz, M.D., Rocío Ruiz, Ph.D., Martiniano Santiago, Ph.D., Esther Berrocoso, Ph.D.

ANESTHESIOLOGY 2024; 141:131–50

EDITOR'S PERSPECTIVE

What We Already Know about This Topic

- Increasing evidence suggests the involvement of the noradrenergic locus coeruleus in the dynamic modulation of nociception
- The role of neuronal projections from the locus coeruleus to the spinal cord and to the rostral anterior cingular cortex in the modulation of neuropathic pain over time is incompletely understood

What This Article Tells Us That Is New

- In an experimental model of chronic constriction nerve injury in rats, a combination of genetic and histologic approaches revealed a biphasic time-dependent role for locus coeruleus neurons in modulating nociceptive responses
- After 2 days of nerve injury, activation of locus coeruleus neurons projecting to spinal cord played a role in attenuating pain-like behavior while activation of locus coeruleus neurons projecting to the rostral anterior cingular cortex amplified nociceptive responses
- After 30 days of nerve injury, only the projections from locus coeruleus neurons to the rostral anterior cingular cortex contributed to the modulation of pain-like behavior in this experimental model

ABSTRACT

Background: Dynamic changes in neuronal activity and in noradrenergic locus coeruleus (LC) projections have been proposed during the transition from acute to chronic pain. Thus, the authors explored the cellular cFos activity of the LC and its projections in conjunction with spontaneous pain-like behavior in neuropathic rats.

Methods: Tyrosine hydroxylase:Cre and wild-type Long–Evans rats, males and females, were subjected to chronic constriction injury (CCI) for 2 (short-term, CCI-ST) or 30 days (long-term, CCI-LT), evaluating cFos and Fluoro-Gold expression in the LC, and its projections to the spinal cord (SC) and rostral anterior cingulate cortex (rACC). These tests were carried out under basal conditions (unstimulated) and after noxious mechanical stimulation. LC activity was evaluated through chemogenetic and pharmacologic approaches, as were its projections, in association with spontaneous pain-like behaviors.

Results: CCI-ST enhanced basal cFos expression in the LC and in its projection to the SC, which increased further after noxious stimulation. Similar basal activation was found in the neurons projecting to the rACC, although this was not modified by stimulation. Strong basal cFos expression was found in CCI-LT, specifically in the projection to the rACC, which was again not modified by stimulation. No cFos expression was found in the CCI-LT $LC_{ipsilateral\ (ipsi)/contralateral\ (contra)}$→SC. Chemogenetics showed that CCI-ST is associated with greater spontaneous pain-like behavior when the LC_{ipsi} is blocked, or by selectively blocking the LC_{ipsi}→SC projection. Activation of the LC_{ipsi} or $LC_{ipsi/contra}$→SC dampened pain-like behavior. Moreover, Designer Receptor Exclusively Activated by Designer Drugs (DREADDs)–mediated inactivation of the CCI-ST LC_{ipsi}→rACC or CCI-LT $LC_{ipsi/contra}$→rACC pathway, or intra-rACC antagonism of α-adrenoreceptors, also dampens pain-like behavior.

Conclusions: In the short term, activation of the LC after CCI attenuates spontaneous pain-like behaviors *via* projections to the SC while increasing nociception *via* projections to the rACC. In the long term, only the projections from the LC to the rACC contribute to modulate pain-like behaviors in this model.

(ANESTHESIOLOGY 2024; 141:131–50)

The locus coeruleus (LC) noradrenergic system is the main source of noradrenaline in the central nervous system, and it is a key brain area involved in pain plasticity.[1–3] Numerous studies indicate that the LC is engaged by acute noxious stimuli or inflammation, promoting feedback inhibition of pain.[4–6] However, recent studies suggest that the LC does not fulfill a uniform role in chronic pain, but rather, it changes dynamically through the activation of specific LC projections while others are silenced as pain

Supplemental Digital Content is available for this article. Direct URL citations appear in the printed text and are available in both the HTML and PDF versions of this article. Links to the digital files are provided in the HTML text of this article on the Journal's Web site (www.anesthesiology.org). Part of the work presented in this article has been presented as a poster at International Association for the Study of Pain, Toronto, Canada, September 19 through 23, 2022; and at European Pain Federation, Dublin, Ireland, April 27 through 30, 2022. I.S.P. and C.L.M. contributed equally to this article.

Submitted for publication July 14, 2023. Accepted for publication March 26, 2024. Published online first on April 10, 2024.

 ANESTHESIOLOGY 2024; 141:131–50. DOI: 10.1097/ALN.0000000000005006

The article processing charge was funded through the authors' institution.

transitions from acute to chronic, contributing to both analgesia and pain.[7] Indeed, 2 days after nerve lesion, we find stronger basal activity in the LC ipsilateral to the side of lesion (LC_{ipsi}) than in the contralateral LC (LC_{contra}), as witnessed through the expression of cFos.[8] Stronger cFos expression was also evident in the LC_{ipsi} neurons projecting to the spinal cord (SC), and similar strong cFos expression was evident after long-term nerve damage (30 days). However, in this latter case, the enhanced cFos expression was bilateral in the LC, and it was also evident in neurons projecting to the rostral anterior cingulate cortex (rACC).[8] The expression of cFos is a common marker for recent cellular activity, reflecting cell activation induced by acute events.[9] For example, acute stress or nociceptive stimulus increases cFos expression in the LC within 1.5 to 2 h of the insult.[10–13] Therefore, the physiologic significance of an increase in cFos 2 days or longer after nerve injury is intriguing. Furthermore, it is unclear whether the critical circuits for the normal processing of acute noxious inputs are disrupted by nerve damage.

It has been proposed that spontaneous strong basal cFos expression might possibly reflect the participation of the LC in processing spontaneous pain. Sensitivity to evoked nociceptive stimuli is enhanced in patients experiencing neuropathic pain, as it is to spontaneous pain. However, while paroxysmal or ongoing spontaneous pain is consistently identified as a major clinical complaint (see review[14]), the underlying mechanisms remain unclear. To further explore this issue, we assessed whether constriction damage to the sciatic nerve alters the activity of LC cells at early and late time points after lesion, both under basal conditions (unstimulated) and after the application of a noxious mechanical stimulus. Furthermore, as the LC is apparently composed of modules that might produce targeted neuromodulation,[2,3,15] we assessed the role of the LC as a whole, and both the LC_{ipsi} or LC_{contra} to the lesion. In addition, we assessed the temporal modulation of pain by examining the descending LC pathway to the SC, as noradrenaline released in the SC suppresses pain-like behaviors.[6,16] We also studied the rACC, an area connected to the LC and implicated in neuropathic pain.[17] These studies were prompted by findings associating bilateral increases in noradrenaline in the prefrontal cortex with long-term neuropathy,[18] suggesting overactivation of the noradrenergic system in prolonged pain conditions. Consequently, cFos expression and Fluoro-Gold (FG; Fluorochrome, USA) staining were explored in the LC of Long–Evans rats subjected to chronic constriction injury (CCI) for 2 days (short-term, CCI-ST) or 30 days (long-term, CCI-LT), analyzing how this responded to noxious mechanical stimuli. Chemogenetics were used to manipulate LC activity and that of the specific LC pathways to the SC or rACC, particularly in relation to spontaneous pain-like behaviors.[8,18] In addition, pharmacologic studies were performed to evaluate the involvement of rACC adrenergic receptors in spontaneous pain-like behaviors.

Materials and Methods

Animals

Transgenic rats were obtained by crossing hemizygous tyrosine hydroxylase–Cre (TH:Cre) transgenic and wild-type (WT) Long–Evans rats at the University of Cádiz (Cádiz, Spain) from founders provided by the Rat Resource and Research Center (Columbia, Missouri; donated by K. Deisseroth, Ph.D.), or WT Long–Evans rats produced in house or obtained commercially from Charles River (Italy) and from Janvier Laboratories (France). Experiments were carried out on male TH:Cre transgenic or on male and female WT Long–Evans rats (300 to 450 g), all maintained at the University of Cadiz under standard laboratory conditions (22°C, 12-h light/dark cycle, lights on 8:00 AM, food and water *ad libitum*). All animal handling and procedures were carried out in accordance with the European Commission (Brussels, Belgium) directive (2010/63/EU) and Spanish law (RD 53/2013) regulating animal

Irene Suárez-Pereira, Ph.D.: Biomedical Research Networking Center for Mental Health (CIBERSAM), Institute of Health Carlos III (ISCIII), Madrid, Spain; Neuropsychopharmacology and Psychobiology Research Group, Department of Neuroscience, Faculty of Medicine, University of Cádiz, Cádiz, Spain; Biomedical Research and Innovation Institute of Cádiz (INIBICA), Puerta del Mar University Hospital, Cádiz, Spain.

Carolina López-Martín, M.Sc.: Biomedical Research Networking Center for Mental Health (CIBERSAM), Institute of Health Carlos III (ISCIII), Madrid, Spain; Neuropsychopharmacology and Psychobiology Research Group, Department of Neuroscience, Faculty of Medicine, University of Cádiz, Cádiz, Spain; Biomedical Research and Innovation Institute of Cádiz (INIBICA), Puerta del Mar University Hospital, Cádiz, Spain.

Carmen Camarena-Delgado, Ph.D.: Biomedical Research and Innovation Institute of Cádiz (INIBICA), Puerta del Mar University Hospital, Cádiz, Spain; IRCCS Humanitas Research Hospital, Milan, Italy; Institute of Neuroscience (IN-CNR), National Research Council of Italy, Milan, Italy.

Meritxell Llorca-Torralba, Ph.D.: Biomedical Research Networking Center for Mental Health (CIBERSAM), Institute of Health Carlos III (ISCIII), Madrid, Spain; Biomedical Research and Innovation Institute of Cádiz (INIBICA), Puerta del Mar University Hospital, Cádiz, Spain; Neuropsychopharmacology and Psychobiology Research Group, Department of Cell Biology and Histology, University of Cádiz, Cádiz, Spain.

Francisco González-Saiz, M.D.: Biomedical Research Networking Center for Mental Health (CIBERSAM), Institute of Health Carlos III (ISCIII), Madrid, Spain; Department of Neuroscience, Faculty of Medicine, University of Cádiz, Cádiz, Spain; Community Mental Health Unit of Villamartin, University Hospital of Jerez de la Frontera, Cádiz, Spain.

Rocío Ruiz, Ph.D.: Department of Biochemistry and Molecular Biology, Faculty of Pharmacy, Institute of Biomedicine of Sevilla (IBiS) - University Hospital Virgen del Rocío/CSIC/University of Sevilla, Sevilla, Spain.

Martiniano Santiago, Ph.D.: Department of Biochemistry and Molecular Biology, Faculty of Pharmacy, Institute of Biomedicine of Sevilla (IBiS) - University Hospital Virgen del Rocío/CSIC/University of Sevilla, Sevilla, Spain.

Esther Berrocoso, Ph.D.: Biomedical Research Networking Center for Mental Health (CIBERSAM), Institute of Health Carlos III (ISCIII), Madrid, Spain; Neuropsychopharmacology and Psychobiology Research Group, Department of Neuroscience, Faculty of Medicine, University of Cádiz, Cádiz, Spain; Biomedical Research and Innovation Institute of Cádiz (INIBICA), Puerta del Mar University Hospital, Cádiz, Spain.

research. Furthermore, all experimental protocols were approved by the Committee for Animal Experimentation at the University of Cadiz. The study was conducted and the data reported in accordance with the Animal Research: Reporting of In Vivo Experiments (ARRIVE) guidelines.[19]

Neuropathic Pain Model

CCI of the sciatic nerve was used as a model of neuropathic pain.[20,21] Rats were anesthetized with isoflurane (induction with 3 to 4% and maintenance with 1.5 to 2.5%), and the left sciatic nerve was then exposed at the mid-thigh level, proximal to the sciatic trifurcation. Four chrome gut (4–0) ligatures were tied loosely around the nerve, separated by 1.0 to 1.5 mm so as not to compromise the vascular supply. The overlying layers of muscle were then closed with 4–0 nonabsorbable silk thread, and the skin was sutured with 2–0 silk thread. Sham operations were performed in the same manner but without nerve ligation. The experimental procedures were carried out 2 (ST) and 30 (LT) days after CCI.

Experimental Design and Groups

All animals used in this study were initially randomized into groups that were assigned different treatments. In the experiments involving female rats, they were initially assigned randomly to the different groups, and subsequently, their hormonal status was assessed by examining vaginal smears while they were under anesthesia before applying noxious hind paw stimulation.[22] All stages of the estrous cycle were represented in each group, as determined by vaginal cytology. Before the behavioral experiments, all the animals underwent initial training and were habituated to both the experimental room and handling. All the experiments and the analysis of the data were performed blind to the group and treatment assignments. Furthermore, power analyses were performed with G*Power[23] (Heinrich-Heine-Universität Düsseldorf, Düsseldorf, Germany) to determine the minimum sample size required for the experiments in order to detect a significant effect using two-tailed *t* tests at an α level = 0.05, power = 0.80, and effect size based on similar published studies of cFos expression in the LC[8] and paw flinches in spontaneous pain tests.[24] Detailed sample size tables for each figure (figs. 1 through 7) are shown in Supplemental Digital Content 2 (Supplemental Tables 1 through 7, https://links.lww.com/ALN/D532). Some experimental units or data points were excluded from the experiment or statistical analysis if histologic verification indicated retrograde tracer injection or the site of catheter/cannula placement was inaccurate, or if there was no Designer Receptor Exclusively Activated by Designer Drugs (DREADDs) expression in the LC. Furthermore, a Grubbs's statistical test was employed to detect outliers within the dataset. These exclusion criteria were predefined before conducting the analysis.

Schemes representing the experimental procedure are shown in each figure. In general, CCI was induced in male and female adult Long–Evans rats at two different time points after nerve injury: 2 days (CCI-ST) and 30 days (CCI-LT). As control groups, rats were subjected to a sham surgical procedure (sham group) or left unoperated (naive group). To explore changes in LC activity and its projections over time, and with respect to noxious stimulation, CCI and control animals (sham or naive) were initially randomized into the following experimental groups: Stim(–), unstimulated; or Stim(+), stimulated. Alternatively, for the chemogenetic modulation of global noradrenergic LC neuron activity or of specific noradrenergic LC projections, adeno-associated virus (AAV)–Gi–mCherry (DREADDs for chemogenetic inhibition), AAV-Gs-mCherry (DREADDs for chemogenetic activation), or AAV-mCherry (control virus) was injected into the LC_{ipsi} and/or LC_{contra} of TH:Cre rats. Clozapine-N-oxide (CNO, designer ligand) was administered *via* intraperitoneal injection, or locally (intrathecal or intra-rACC) *via* microinjection into the target site 20 min before performing the behavioral tests. In all these experiments, a group administered the vehicle alone was included as a control (saline [Sal] group). Finally, for the pharmacologic blockade of adrenoreceptors in the rACC, a cannula was implanted bilaterally into the rACC of all experimental rats, and the drugs were administered 30 or 20 min before performing the behavioral tests (see section "Drugs"). Similarly, a group administered with the vehicle alone was included as a control (saline group) in these experiments.

Noxious Hind Paw Stimulation

The hind paw of rats was stimulated by applying pinched pressure to the ipsilateral (left) hind paw (600 g, 5 min) using a Analgesy-Meter (Ugo Basile, Italy), defined as a mechanical noxious stimulation, to enhance cFos expression. This stimulus was administered under mild anesthesia with sodium pentobarbital (50 mg/kg, intraperitoneally).[26] Two hours after noxious stimulation, all the rats were anesthetized deeply with an overdose of sodium pentobarbital, and they received a transcardial perfusion with saline, followed by 4% paraformaldehyde (PFA) in 0.1 M phosphate buffer (PB), after which their SC and brain were removed.[27]

DREADDs Approaches

DREADDs approaches were carried out as indicated previously, whereby strong colocalization between mCherry and noradrenergic neurons was found in the LC of TH:Cre rats. For methodologic validation of the DREADDs approach, see Llorca-Torralba *et al.*,[8,28] as well as Supplemental Figures 1 and 2 (Supplemental Digital Content 1, https://links.lww.com/ALN/D531).

Stereotaxic Surgery. The following vectors were used in these studies: DREADDs (Virus Vector Core, Gene Therapy Center Vector Core at the University of North Carolina, USA); AAV2/hSyn-DIO-hM4D(Gi)-mCherry

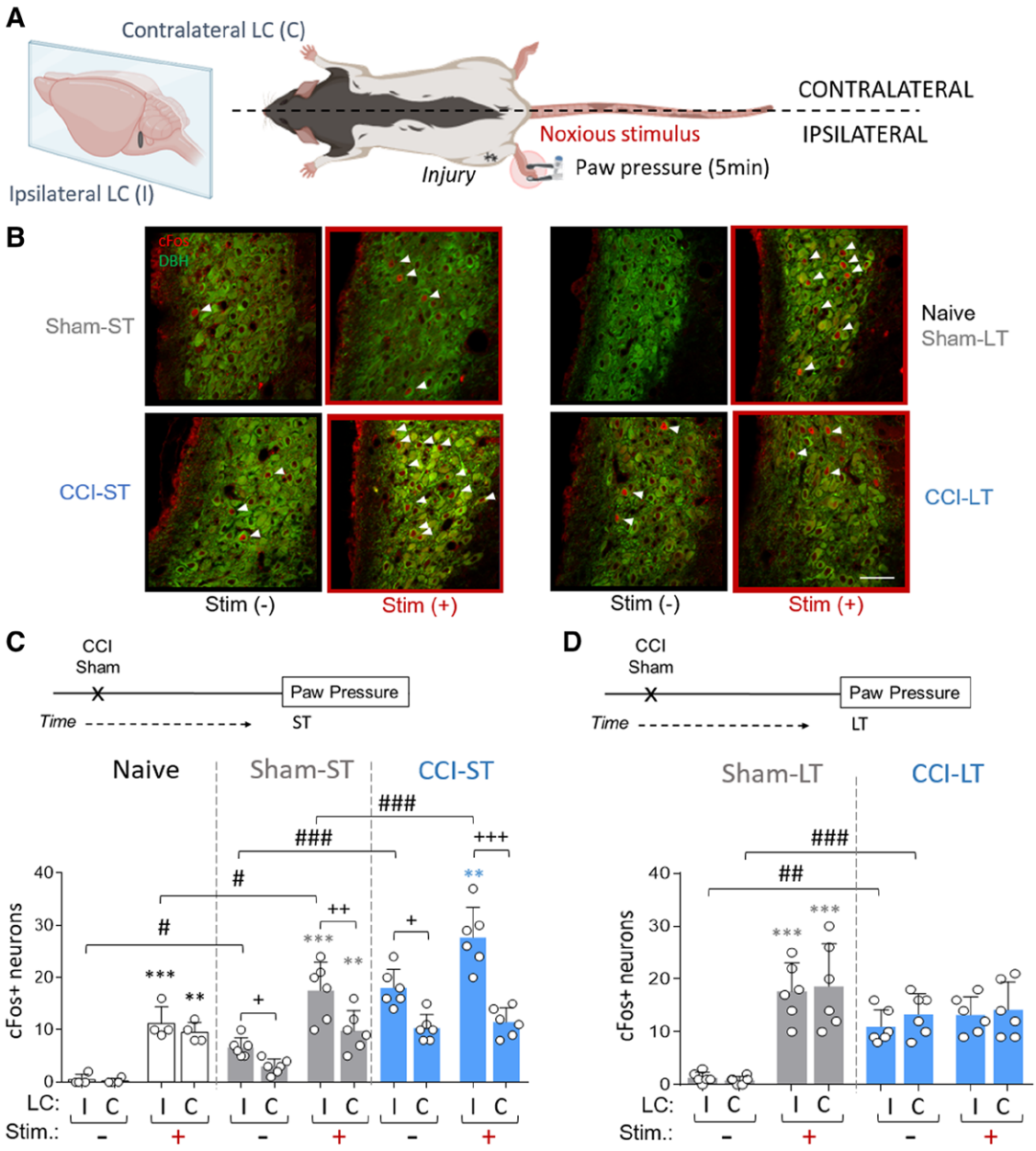

Fig. 1. Study of locus coeruleus (LC) activation over time after neuropathy in unstimulated and stimulated male rats. (*A*) Scheme representing the experimental procedure. The paw ipsilateral to the injured one was stimulated in anesthetized rats by paw compression using an Analgesy-Meter (Ugo Basile, Italy; 600 g, 5 min). The terms ipsilateral and contralateral are relative to the chronic constriction injury (CCI). (*B*) Representative immunohistochemistry of cFos labeled neurons in the ipsilateral central LC (–9.72 to –9.96 from bregma[25]) in conditions of no stimulation (Stim[–], *black borders*) or stimulation (Stim[+], *red borders*) in naive, sham–short-term (ST), sham–long-term (LT), CCI-ST, and CCI-LT wild-type rats (*scale bar*, 100 μm: cFos, *red*; dopamine beta-hydroxylase [DBH], *green*). The *white arrows* illustrate examples of DBH-positive cells with cFos-positive nuclei in LC. (*C*) Experimental timeline of neuropathy and ST (2 days) quantification of the cFos-positive neurons in the central ipsilateral (I) and contralateral (C) LC of naive, sham-ST, and CCI-ST rats without stimulation (Stim[–]) or after applying a noxious stimulus (Stim[+]). The mean + SD neurons per slice are shown (each point represents an individual rat; n = 4–6 animals/group): $^{**}P < 0.01$, $^{***}P < 0.001$ *vs.* Stim(–); $+P < 0.05$, $++P < 0.01$, $+++P < 0.001$ *vs.* LC_{ipsi}; $\#P < 0.05$, $\#\#\#P < 0.001$ *vs.* naive or sham-ST (three-way ANOVA with Tukey *post hoc* test between naive and sham-ST groups, and between sham-ST and CCI-ST groups). (*D*) Experimental timeline of neuropathy and LT (30 days) quantification of the cFos-positive neurons in the central ipsilateral (I) and contralateral (C) LC of sham-LT and CCI-LT rats without stimulation (Stim[–]) or with noxious stimulation (Stim[+]). The mean + SD neurons per slice are shown (each point represents an individual rat; n = 6 animals/group): $^{***}P < 0.001$ *vs.* Stim(–); $\#\#P < 0.01$, $\#\#\#P < 0.001$ *vs.* sham-LT (three-way ANOVA with Tukey *post hoc* test).

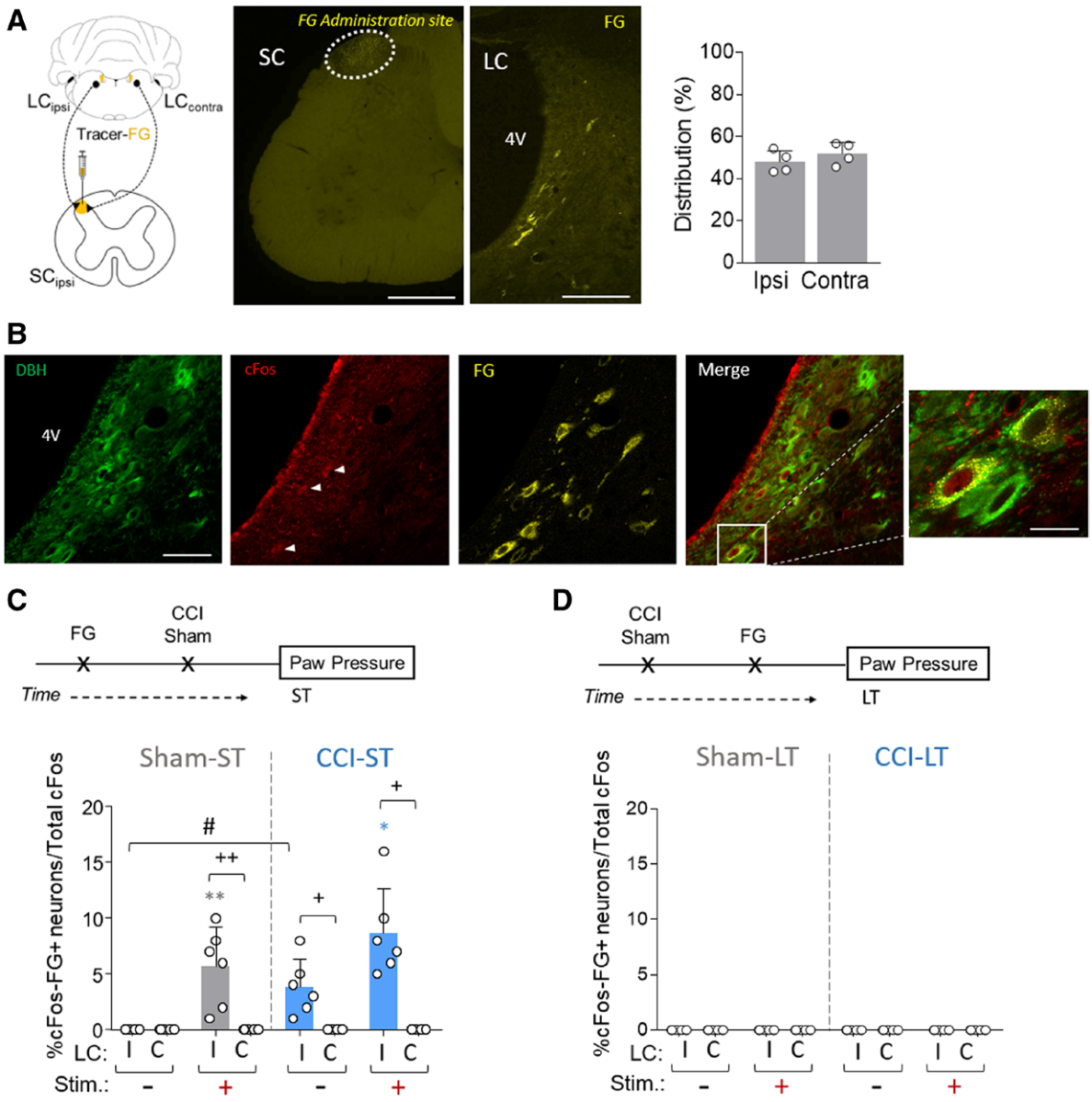

Fig. 2. Study of the activation of the locus coeruleus (LC)→spinal cord (SC) pathway over time after neuropathy in unstimulated and stimulated male rats. (*A*) Scheme of the retrograde Fluoro-Gold (FG; Fluorochrome, USA) tracer strategy and representative images (*scale bar*, 500 μm) of FG administration site and LC neurons that project to the ipsilateral spinal cord (SC) in wild-type rats. Distribution of FG labeling in ipsilateral (ipsi) and contralateral (contra) LC neurons (mean + SD of the number of neurons per slice; each point represents an individual rat; n = 4 animals: Student's *t* test). (*B*) Representative immunofluorescence of the central LC (–9.72 to –9.96 from bregma[25]) showing the DBH, cFos, and FG expression, as well as a merged image. The *white arrows* illustrate examples of cFos-positive cells, and the *inset* shows an example of cFos/FG-labeled DBH-positive neurons (*scale bar*, 100 μm: DBH, *green*; cFos, *red*; FG, *yellow*). (*C*) Experimental timeline of neuropathy and short-term (ST, 2 days) quantification of the cFos/FG labeled neurons in the central ipsilateral (I) and contralateral (C) LC of sham-ST and CCI-ST rats without stimulation (Stim[–]) or with noxious stimulation (Stim[+]). The mean + SD neurons per slice are shown (each point represents an individual rat; n = 6 animals/group): *$P < 0.05$, **$P < 0.01$ *vs.* Stim(–); +$P < 0.05$, ++$P < 0.01$ *vs.* LC$_{ipsi}$; #$P < 0.05$ *vs.* sham-ST (three-way ANOVA with Tukey *post hoc* test). (*D*) Experimental timeline of neuropathy and long-term (LT, 30 days) quantification of the cFos/FG-labeled neurons in the central ipsilateral (I) and contralateral (C) LC of sham-LT and CCI-LT rats without stimulation (Stim[–]) or with noxious stimulation (Stim[+]). The mean + SD neurons per slice are shown (each point represents an individual rat; n = 6 animals/group): non-significant differences (three-way ANOVA with Tukey *post hoc* test). CCI, chronic constriction injury; DBH, dopamine beta-hydroxylase; 4V, fourth ventricle.

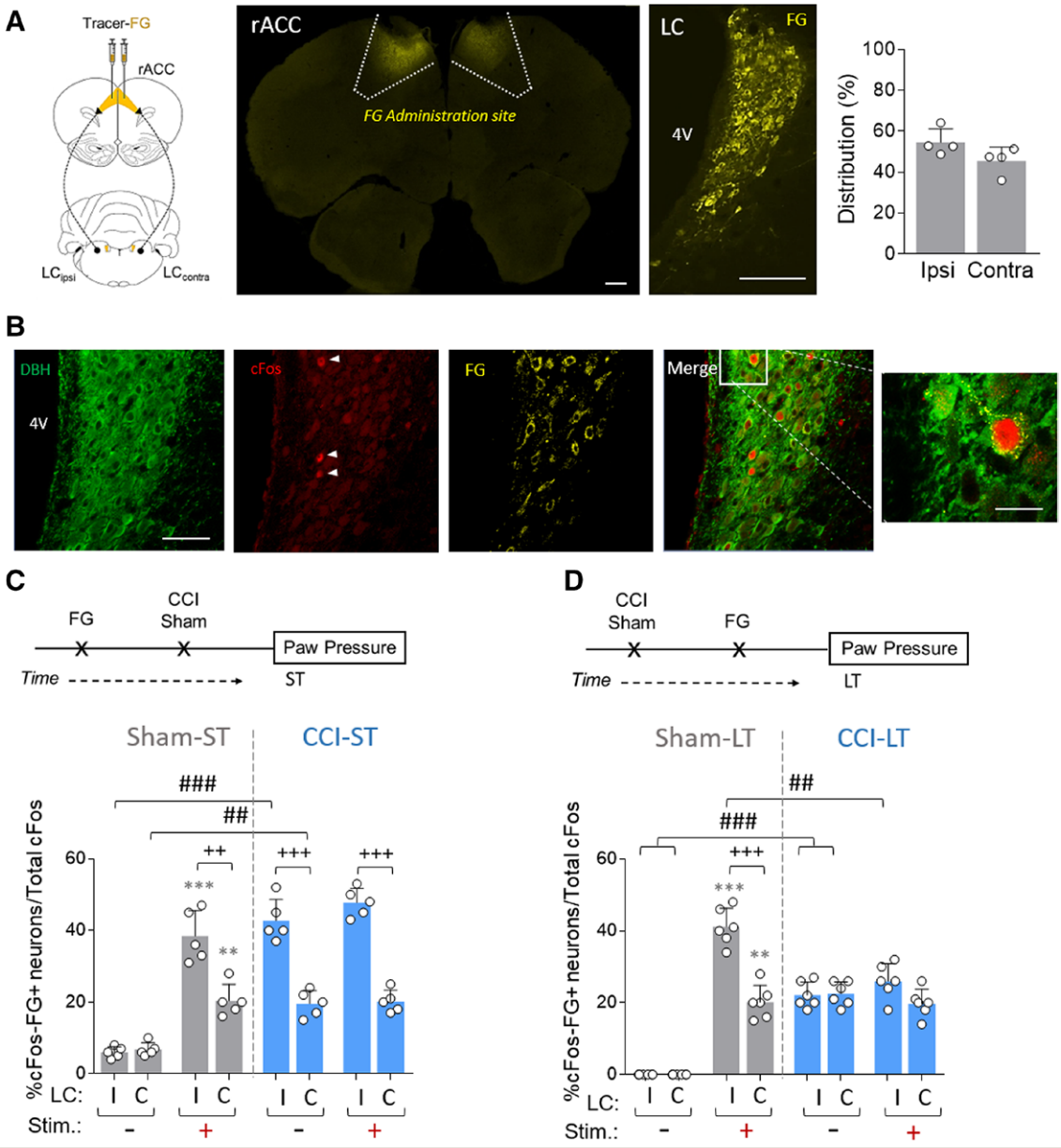

Fig. 3. Study of the activation of the locus coeruleus (LC)→rostral anterior cingulate cortex (rACC) pathway over time after neuropathy in unstimulated and stimulated male rats. (*A*) Cartoon of the retrograde Fluoro-Gold (FG; Fluorochrome, USA) tracer strategy targeting LC neurons that project to the bilateral rACC and representative images (*scale bar*, 500 μm) of FG administration site and LC neurons that project bilaterally to the rACC in wild-type rats. The distribution of FG label in the ipsilateral (ipsi) and contralateral (contra) LC neurons was evaluated (mean + SD of the number of neurons per slice; each point represents an individual rat; n = 4 animals: Student's *t* test). (*B*) Representative immunofluorescence of the central LC (–9.72 to –9.96 from bregma[25]) showing the DBH, cFos, and FG expression, as well as a merged image. The *white arrows* illustrate examples of cFos-positive cells, and the *inset* shows an example of cFos/FG-labeled DBH-positive neurons (*scale bar*, 100 μm: DBH, *green*; cFos, *red*; FG, *yellow*). (*C*) Experimental timeline of neuropathy and short-term (ST, 2 days) quantification of the cFos/FG-labeled neurons of the central ipsilateral (I) and contralateral (C) LC of sham-ST and CCI-ST rats without stimulation (Stim[–]) or after applying a noxious stimulus (Stim[+]). The mean + SD neurons per slice are shown (each point represents an individual rat; n = 5 animals/group): $^{**}P < 0.01$, $^{***}P < 0.001$ *vs.* (Stim[–]); $^{++}P < 0.01$, $^{+++}P < 0.001$ *vs.* LC_{ipsi}; $^{\#\#}P < 0.01$, $^{\#\#\#}P < 0.001$ *vs.* sham-ST (three-way ANOVA with Tukey *post hoc* test). (*D*) Experimental timeline of neuropathy and long-term (LT, 30 days) quantification of the cFos/FG-labeled neurons of the central ipsilateral (I) and contralateral (C) LC of sham-LT and CCI-LT rats without stimulation (Stim[–]) or with noxious stimulation (Stim[+]). The mean + SD neurons per slice are shown (each point represents an individual rat; n = 5 or 6 animals/group): $^{**}P < 0.01$, $^{***}P < 0.001$ *vs.* (Stim[–]); $^{+++}P < 0.001$ *vs.* LC_{ipsi}; $^{\#\#}P < 0.01$, $^{\#\#\#}P < 0.001$ *vs.* sham-LT (three-way ANOVA with Tukey *post hoc* test). CCI, chronic constriction injury; DBH, dopamine beta-hydroxylase; 4V, fourth ventricle.

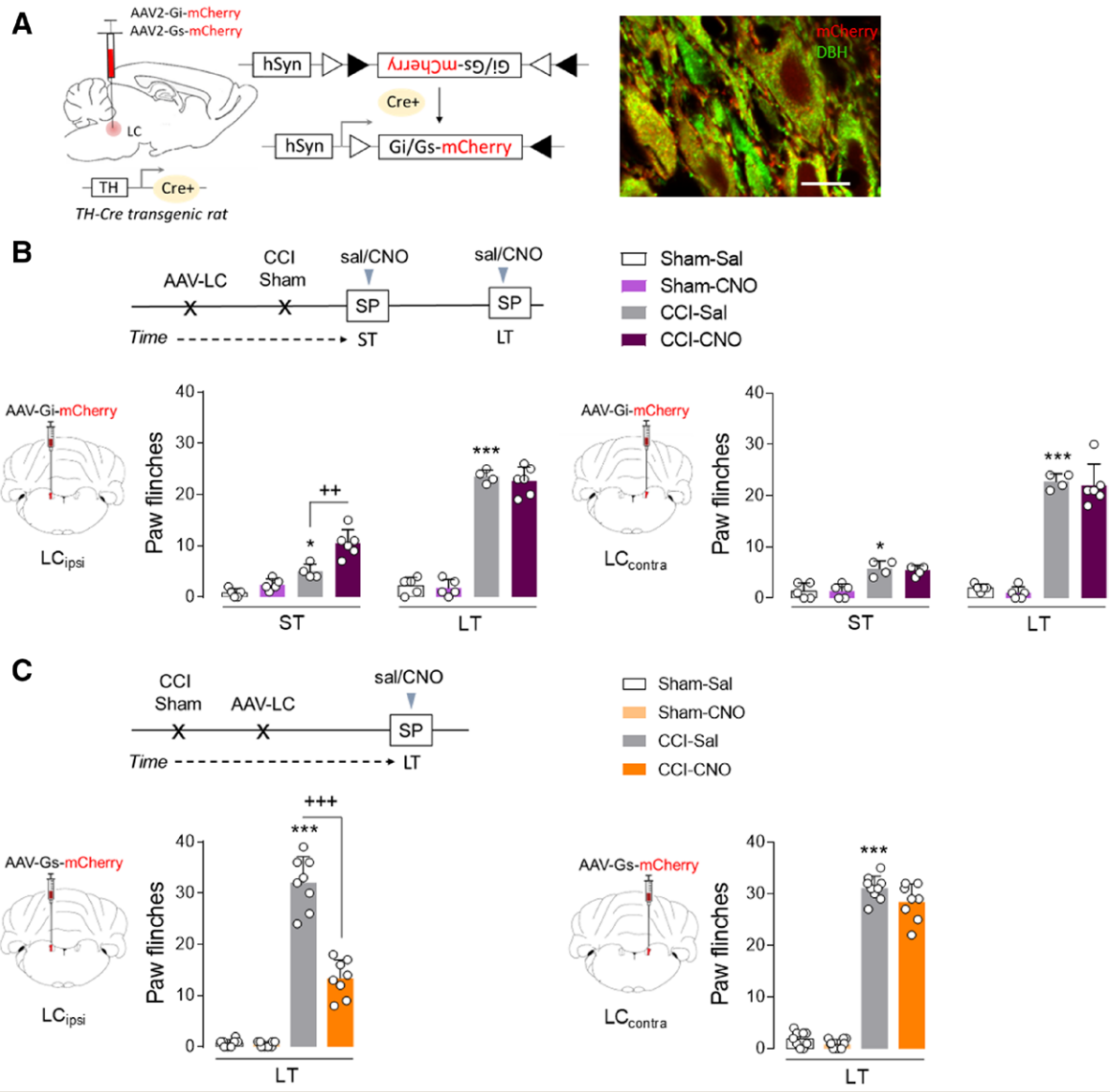

Fig. 4. Effect of chemogenetic inhibition and activation of the ipsilateral and contralateral locus coeruleus (LC) on spontaneous pain-like behavior at different times after nerve injury. (*A*) Scheme of the noradrenergic LC inhibition or activation using the DREADD strategy in TH:Cre male rats and representative immunofluorescence image (*scale bar*, 10 μm) of mCherry expression in the noradrenergic LC neurons (DBH, *green*; mCherry, *red*). (*B*) Experimental timeline of neuropathy and quantification of the short-term (ST, 2 days) and long-term (LT, 30 days) ipsilateral paw flinches of sham and CCI rats in the spontaneous pain test after ipsilateral LC (LC_{ipsi}) or contralateral LC (LC_{contra}) noradrenergic inhibition by CNO (1 mg/kg intraperitoneal, mean + SD, each point represents an individual rat; n = 4–6 animals/group: $^{*}P < 0.05$, $^{***}P < 0.001$, *vs.* sham-Sal; $^{++}P < 0.01$ *vs.* CCI-Sal, three-way repeated measures ANOVA with Tukey *post hoc* test). (*C*) Experimental timeline of neuropathy and long-term (LT, 30 days) quantification of the ipsilateral paw flinches of sham and CCI rats in the spontaneous pain test after ipsilateral LC (LC_{ipsi}) or contralateral LC (LC_{contra}) noradrenergic activation by CNO (1 mg/kg intraperitoneal, mean + SD, each point represents an individual rat; n = 8 or 9 animals/group: $^{***}P < 0.001$ *vs.* sham-Sal; $^{+++}P < 0.001$ *vs.* CCI-Sal, Kruskal–Wallis test followed by Mann–Whitney U test). AAV, adeno-associated virus; CCI, chronic constriction injury; CNO, clozapine N-oxide; DBH, dopamine beta-hydroxylase; DREADD, Designer Receptor Exclusively Activated by Designer Drug; Sal, saline; SP, spontaneous pain-like test; TH, tyrosine hydroxylase.

(hM4D[Gi]-DREADD) inhibitor virus, titer 3×10^{12} vg/ml, 1.4 μl/ LC; AAV2/hSyn-DIO-rM3D(Gs)-mCherry (rM3D[Gs]-DREADD) activator virus, titer 3×10^{12} vg/ml, 1.4 μl/LC; and AAV2/hSyn-DIO-mCherry (control-DREADD), titer 5.6×10^{12} vg/ml, 1.4 μl/LC. This control vector contained a mCherry reporter protein without the DREADD reporter.

DREADDs vectors were injected into the LC of TH:Cre rats anesthetized (intraperitoneally) with ketamine (100 mg/kg, Richter Pharma, Spain) and xylazine (20 mg/

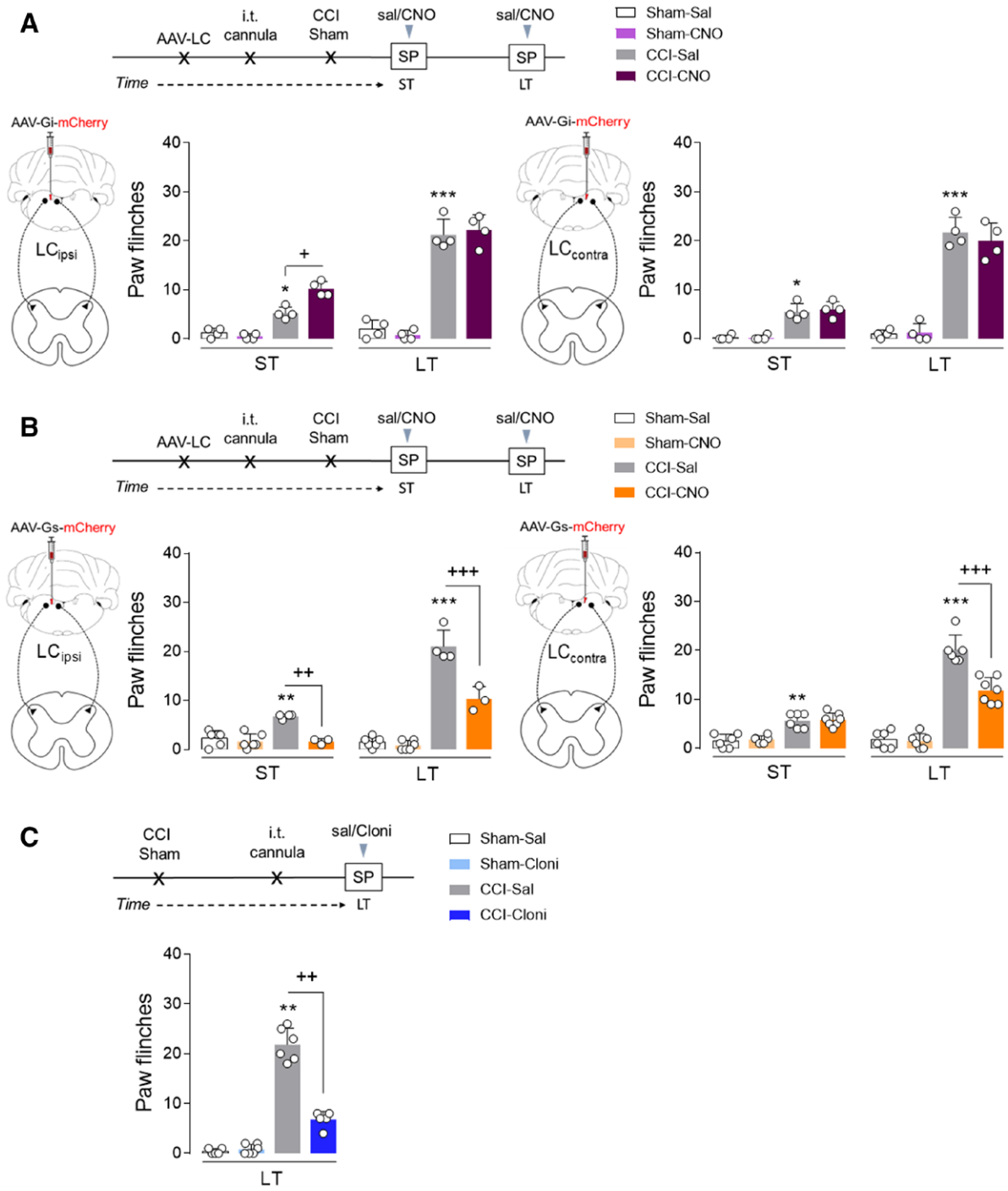

Fig. 5. Effect of chemogenetic inhibition and activation of ipsilateral and contralateral locus coeruleus (LC)→spinal cord (SC) pathway on spontaneous pain-like behavior over time after nerve injury. (*A*) Experimental timeline of LC_{ipsi}-SC or LC_{contra}-SC pathway inhibition at short-term (ST, 2 days) and long-term (LT, 30 days) after neuropathy using the DREADD strategy in male TH:Cre rats. Quantification of the ipsilateral paw flinches of sham and CCI rats in the spontaneous pain-like test after ipsilateral LC (LC_{ipsi}) or contralateral LC (LC_{contra}) noradrenergic inhibition by CNO (3 μM intrathecal, mean + SD, each point represents an individual rat; n = 4 animals/group: $^{*}P < 0.05$, $^{***}P < 0.001$, *vs.* sham-Sal; $^{+}P < 0.05$ *vs.* CCI-Sal, three-way repeated measures ANOVA with Tukey *post hoc* test). (*B*) Experimental timeline of LC_{ipsi}→SC or LC_{contra}→SC pathway activation in the short-term (ST, 2 days) and long-term (LT, 30 days) after neuropathy using the DREADD strategy in TH:Cre rats. Quantification of the ipsilateral paw flinches of sham and CCI rats in the spontaneous pain test after ipsilateral LC (LC_{ipsi}) or contralateral LC (LC_{contra}) noradrenergic activation by CNO (3 μM intrathecal, mean + SD, each point represents an individual rat; n = 3–7 animals/group: $^{**}P < 0.01$, $^{***}P < 0.001$ *vs.* sham-Sal; $^{++}P < 0.01$, $^{+++}P < 0.001$ *vs.* CCI-Sal, three-way repeated measures ANOVA with *(Continued)*

kg, Calier Laboratory, S.A., Spain), which were placed into a stereotaxic frame with the skull level along both the antero-posterior (AP) and medio-lateral (ML) axis for precise targeting. Cranial windows were opened above the LC coordinates (AP, −3.2 mm; ML, ±1.3 mm; dorso-ventral [DV], 6.2 mm), with the head oriented at a 15-degree angle to the horizontal plane. After injection, the wound was cleaned with 0.9% saline and disinfected with iodine polyvidone, and the skin was sutured with 4-0 nonabsorbable silk thread. To enhance vector expression, the behavioral studies were carried out 3 weeks after the injections.

Viral Expression. Animals were perfused with PFA (4%) at the end of the experiments, and their brains were collected and processed[28,29] to verify the viral injection site and the expression of mCherry in the LC by immunofluorescence. All the LC sections (30 μm) were incubated for 48 h at 4°C with an antibody against red fluorescent protein (1:500 [5F8], Chromotek, Germany) and mouse antidopamine beta hydroxylase (DBH, 1:1,000, Merck Chemicals & Life Science S.A., Spain). Subsequently, the antibodies were detected with a biotinylated donkey antirat antibody (1:200, Jackson ImmunoResearch Europe, United Kingdom), which was visualized with Alexa Fluor 568 streptavidin or a donkey antimouse Alexa Fluor 488 (1:1,000, Invitrogen, USA). The sections were then washed and coverslipped in fluoro-gel aqueous mounting medium, and the images were acquired on a Zeiss LSM 900 Confocal microscope with Airyscan 2 (Carl Zeiss Microscopy GmbH, Germany). The selective expression of DREADD was also assessed in the A5 noradrenergic nucleus and ventral tegmental area, the latter probed with a rabbit anti-TH primary antibody (1:1,000) that was visualized with a donkey antirabbit Alexa Fluor 488 (Invitrogen, USA).

Tracer Approach

FG was used as a retrograde tracer (4%/0.4 μl) for the rACC or SC. For FG injections at the lumbar level of the SC,[8] rats were anesthetized with sodium pentobarbital (50 mg/kg, intraperitonally, Vetoquinol S.A., Spain), and local analgesia was administered subcutaneously with carprophen (10 mg/kg, Zoetis, Spain) and bupivacaine (2 mg/kg, B. Braun Medical S.A., Spain). Additional doses of pentobarbital were administered as necessary. Rats were placed in a stereotaxic frame, and a laminectomy was performed at the level of the T12–L2 vertebrae to expose the L4–L6 segments of the SC. The dura was then removed, and FG was administered at four sites along the ipsilateral L4–L6 dorsal horn of the SC (SC_{ipsi}). After FG injection, the skin was closed with staples, and the wound was cleaned with 0.9% saline and disinfected with iodine polyvidone. In another set of experiments, the FG was microinjected unilateral or bilaterally into the rACC according to the same stereotaxic surgery performed in the DREADD experiments (see section "DREADDs Approaches").[8] The target coordinates for rACC were AP + 3.0 mm, ML ± 1.0 mm, and DV 1.2 mm, with the head oriented at a 0-degree angle to the horizontal plane. To enhance tracer expression, the neuroanatomical studies were carried out 4 days after the injections, and the location of the FG injection site was verified to be within the SC and rACC in all the animals studied. Sequential SC and rACC (40 μm) coronal sections were visualized directly on an Olympus BX60 fluorescence microscope equipped with an Olympus DP74 camera (Spain). After verification, the animals in which the FG injection was not appropriately located in the target area were excluded from the analysis.

rACC Cannula Implantation

For intra-rACC drug administration, cannulae were implanted by stereotaxic surgery.[8] The rats were anesthetized with an intraperitoneal injection of ketamine (100 mg/kg) and xylazine (20 mg/kg), and then placed in a stereotaxic frame. The cannulae were implanted bilaterally into the rACC (AP + 3.0 mm, ML ± 1.0 mm, and DV 1.2 mm) with the head oriented at a 0° angle to the horizontal plane. The cannulae were fixed in place with dental cement and four anchor screws, and maintained closed by inserting a stainless steel wire until the test session. After cannula implantation, the rats were allowed to recover for 1 week before the behavioral tests began. To verify cannula placement, 0.5 μl Pontamine Sky Blue (Sigma–Aldrich, Spain) was injected into the intra-rACC just before the animals were sacrificed. Sequential coronal sections (40 μm) of the rACC were ultimately obtained on a Sliding Microtome (Microm HM 450, Fisher Scientific SL, Spain) coupled to BFS-MP freezing stage (Physitemp Instruments, USA). After verification, the animals in which the cannula was not appropriately located in the target area were excluded from the analysis (Supplemental Figures 3, 4, and 5, Supplemental Digital Content 1, https://links.lww.com/ALN/D531).

Intrathecal Catheter Installation

For intrathecal drug injection, a PE-10 catheter (0.61 mm diameter) was implanted into the lumbar SC under isoflurane anesthesia.[30] An incision was made in the skin, and a cannula (20-gauge, 0.9 × 40 mm) was introduced

Fig. 5. *(Continued)* Tukey *post hoc* test). (*C*) Experimental timeline of neuropathy and long-term (LT, 30 days) quantification of the ipsilateral paw flinches of sham and CCI rats in the spontaneous pain test after clonidine (20 μg intrathecal) administration (mean + SD, each point represents an individual rat; n = 5 or 6 animals/group: $^{**}P < 0.01$ *vs.* sham-Sal; $^{++}P < 0.01$ *vs.* CCI-Sal, Kruskal–Wallis test followed by Mann–Whitney U test). AAV, adeno-associated virus; CCI, chronic constriction injury; Cloni, clonidine; CNO, clozapine N-oxide; DREADD, Designer Receptor Exclusively Activated by Designer Drug; Sal, saline; SP, spontaneous pain; TH, tyrosine hydroxylase.

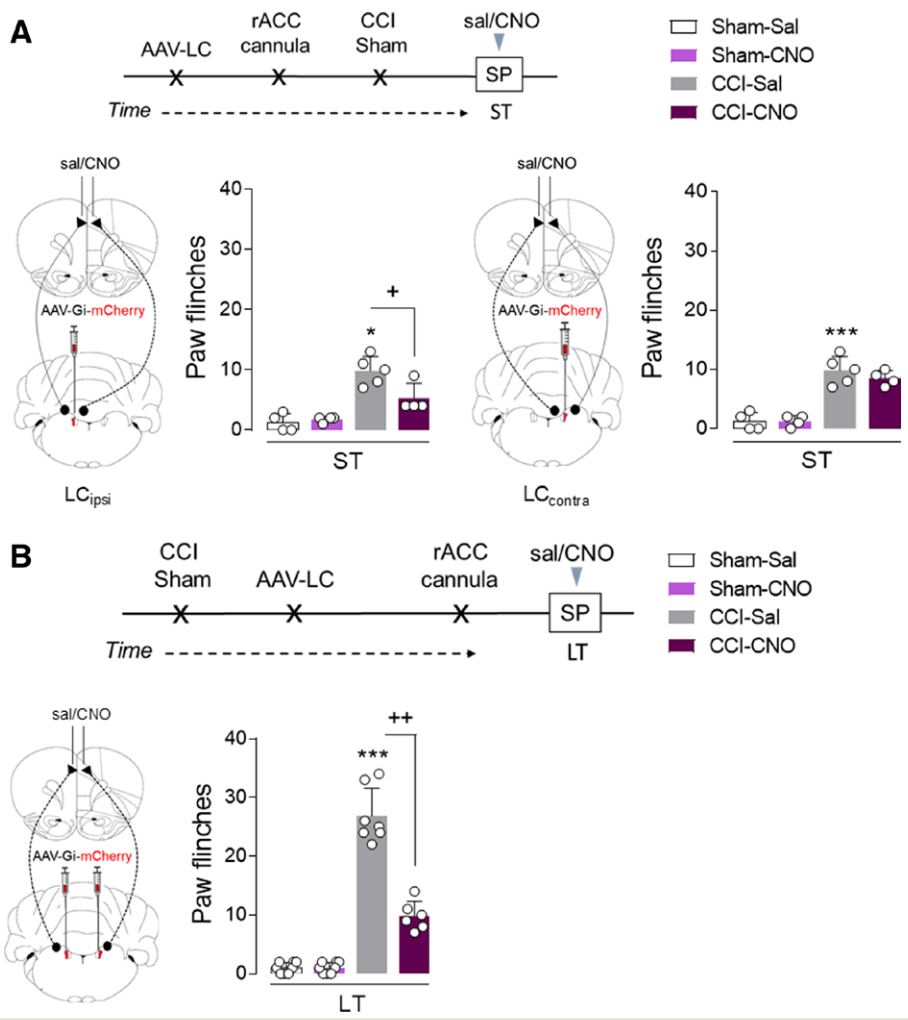

Fig. 6. Effect of chemogenetic inhibition of the locus coeruleus (LC)→rostral anterior cingulate cortex (rACC) pathway on spontaneous pain-like behavior over time after nerve injury. (*A*) Experimental timeline of LC_{ipsi}→rACC or LC_{contra}→rACC pathway inhibition in the short-term (ST, 2 days) after neuropathy using the DREADD strategy in male TH:Cre rats. Quantification of the ipsilateral paw flinches of sham and CCI rats in the spontaneous pain test after ipsilateral LC (LC_{ipsi}) or contralateral LC (LC_{contra}) noradrenergic inhibition by bilateral intra-rACC CNO (3 μM) administration (mean + SD, each point represents an individual rat; n = 4 or 5 animals/group): $^{*}P < 0.05$, $^{***}P < 0.001$ *vs.* sham-Sal; $^{+}P < 0.05$ *vs.* CCI-Sal (Kruskal–Wallis test followed by Mann–Whitney U test or two-way ANOVA with Tukey *post hoc* test, respectively). (*B*) Experimental timeline of LC-rACC pathway inhibition in the long-term (LT, 30 days) after neuropathy using the DREADD strategy in TH:Cre rats. Quantification of the ipsilateral paw flinches of sham and CCI rats in the spontaneous pain test after bilateral LC noradrenergic inhibition by intra-rACC CNO (3 μM) administration (mean + SD, each point represents an individual rat; n = 6–8 animals/group): $^{***}P < 0.001$, *vs.* sham-Sal; $^{++}P < 0.01$ *vs.* CCI-Sal (Kruskal–Wallis test followed by Mann–Whitney U test). AAV, adeno-associated virus; CCI, chronic constriction injury; CNO, clozapine N-oxide; DREADD, Designer Receptor Exclusively Activated by Designer Drug; SP, spontaneous pain-like test; TH, tyrosine hydroxylase.

in a slightly medial cranial direction along the surface of L6 up to L5. The catheter was then introduced from the end of the cannula until it reached the caudal rib level, at which point the cannula was removed. Correct placement of the catheter was confirmed by a tail flick, retraction of the leg, or the reflux of cerebrospinal fluid. The catheter was first fixed onto the surface of the lumbar musculature, and the rest was passed subcutaneously along the spine, appearing through the skin in the occipital region. Lidocaine (4%/15 μl, intrathecally) was administered to verify the correct placement of the intraspinal cannula over time (CCI-ST and -LT), observing immediate motor paralysis of the posterior third of the animal that lasted for about 10 to 20 min. Those animals that did not show motor paralysis were not included in the behavioral tests. After catheter implantation, rats were allowed to recover for 1 week before the behavioral tests began.

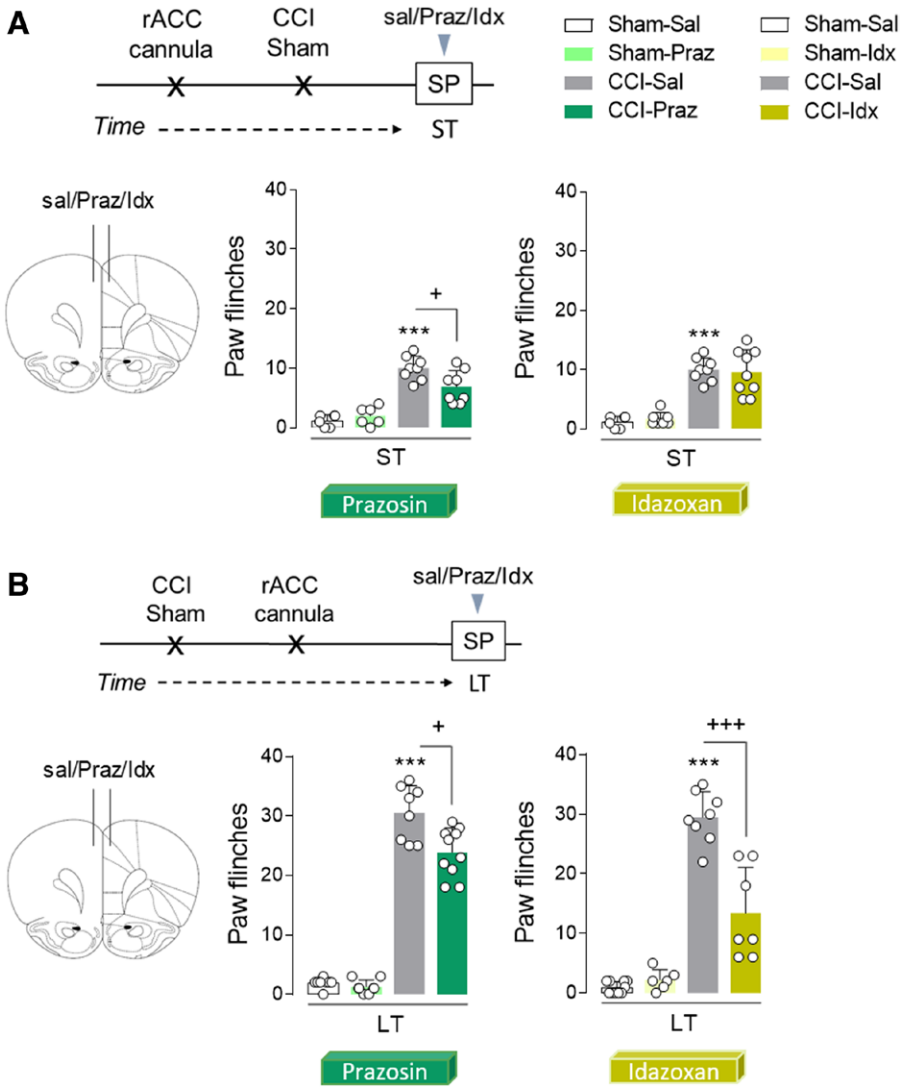

Fig. 7. Effect of pharmacologic blockade of adrenoreceptor activity in the rostral anterior cingulate cortex (rACC) on spontaneous pain-like behavior over time after nerve injury. (*A*) Experimental timeline and cartoon of the pharmacologic inhibition of α1-adrenoreceptors (prazosin, Praz) or α2-adrenoreceptors (idazoxan, Idx) in the rACC of wild-type male rats in the short-term (ST, 2 days) after neuropathy. Quantification of the ipsilateral paw flinches of sham and CCI rats in the spontaneous pain-like test after pharmacologic blockade by bilateral intra-rACC administration of Praz (5 μg; mean + SD, each point represents an individual rat; n = 6–8 animals/group) or Idx (9 μg; mean + SD, each point represents an individual rat; n = 6–9 animals/group): ***$P < 0.001$, *vs.* sham-Sal; +$P < 0.05$, *vs.* CCI-Sal (Kruskal–Wallis test followed by Mann–Whitney U test). (*B*) Experimental timeline and cartoon of the pharmacologic blockade of α-adrenoceptors in the rACC of wild-type rats in the long-term (LT, 30 days) after neuropathy. Quantification of the ipsilateral paw flinches of sham and CCI rats in the spontaneous pain test after pharmacologic blockade by bilateral intra-rACC administration of Praz (5 μg; mean + SD, each point represents an individual rat; n = 8–10 animals/group) or Idx (9 μg; mean + SD, each point represents an individual rat; n = 6–10 animals/group): ***$P < 0.001$, *vs.* sham-Sal; +$P < 0.05$, +++$P < 0.001$ *vs.* CCI-Sal (Kruskal–Wallis test followed by Mann–Whitney U test). CCI, chronic constriction injury; Sal, saline; SP, spontaneous pain-like test.

Drugs

The drugs administered to carry out the behavioral assessment were CNO (Carbosynth, United Kingdom), administered 20 min before the behavioral tests at 1 mg/kg intraperitoneall, 3 μM/20 μl intrathecally, and 3 μM/0.5 μl intra-rACC; clonidine hydrochloride (Cloni, Sigma-Aldrich, Spain), administered 30 min before testing at 20 μg/10 μl intrathecally; prazosin hydrochloride (Praz, Sigma-Aldrich, Spain), administered 30 min before the behavioral tests at 5 μg/0.5 μl intra-rACC; and idazoxan hydrochloride (Idx, Sigma-Aldrich, Spain), administered 20 min before testing at 9 μg/0.5 μl intra-rACC. In all the experiments in which these drugs were used, a group

administered with the vehicle alone was included as a control (saline group). To circumvent the potential side effects associated with systemic CNO administration,[31,32] local CNO administration was used to explore specific pathways: LC→SC and LC→rACC.

Behavioral Assessment

Spontaneous Pain-like Test. All animals were habituated to the experimental room for 30 min in dim light and climate-controlled conditions. The rats were placed into a Plexiglas chamber on a metal grid for 15 min, and a camera (Panasonic HC-V180; Spain) was positioned underneath the chamber to video-record the behavioral test. The sessions were analyzed offline blind to the treatments, and the number of spontaneous paw lifts and flinches was measured over the last 5 min as an index of ongoing pain.[16]

Spontaneous Locomotor Activity. All animals were transported to a light-attenuated experimental room (13 to 14 lux), where they were habituated for 30 min before testing. After drug administration (20 to 30 min), rats were placed individually in the center area of a transparent cage (40 × 40 × 40 cm) that they were allowed to explore freely for 15 min. Free exploratory ambulation of each individual was video-recorded and analyzed offline using a Spontaneous Motor Activity Recording and Tracking (SMART) video system (v3.0, Panlab S.L., Spain). The total distance traveled (centimeters) was measured as an indicator of locomotor activity.[28]

Immunohistochemistry and Histology

The rats' SC and brain were collected and postfixed for 2 h in PFA (4% in 0.1 M PB) and then cryoprotected in 30% sucrose in PB at 4°C.[28,29] Coronal sections were obtained on a Sliding Microtome (Microm HM 450, Fisher Scientific S.L., Spain) coupled to BFS-MP freezing stage (Physitemp Instruments, USA).

FG Expression in LC. FG in the LC_{ipsi} and LC_{contra} projections was evaluated in sequential sections (nine representative 30-μm sections along the rostra-caudal LC axis per animal), incubating them for 48 h at 4°C with a rabbit anti-FG antibody (1:1,000, Merck Chemicals & Life Science S.A., Spain) and a mouse anti-DBH antibody (1:1,000, Merck Chemicals & Life Science S.A., Spain). The antibodies were visualized with a biotinylated donkey antirabbit IgG (1:200, Jackson ImmunoResearch Europe, United Kingdom) followed by Alexa Fluor 488 streptavidin (1:1,000, Invitrogen, USA) or a donkey antimouse Alexa Fluor 568 (1:1,000, Invitrogen, USA). After washing and coverslipping in fluoro-gel aqueous mounting medium, images were acquired on a fluorescent Olympus BX60 microscope equipped with an Olympus DP74 camera (Olympus, Spain). The number of FG-positive cells per LC area in each slice was quantified, and the LC area was measured using the Fiji Image software (USA), representing the data as the mean (+ standard deviation [SD]) per slice, each point corresponding to an individual animal.

cFos Expression in the LC. Activation of the LC_{ipsi} and LC_{contra} after neuropathy (ST and LT), with or without stimulation, was evaluated through the expression of cFos. Moreover, cFos and FG colocalization was assessed in ipsilateral and contralateral LC projections to the SC or rACC. Sequential central LC_{ipsi} and LC_{contra} sections (–9.72 to 9.96 from bregma, 3 × 30 μm slices per animal) were incubated for 48 h at 4°C with a rabbit anti-cFos antibody (1:1,000, Synaptic System, Germany) and a mouse anti-DBH antibody (1:1,000, Merck Chemicals & Life Science S.A., Spain). Antibody binding was detected with a biotinylated donkey antirabbit IgG (1:200, Jackson ImmunoResearch Europe, United Kingdom) and then visualized with Alexa Fluor 488 streptavidin (1:1,000, Invitrogen, USA) or an Alexa Fluor 568 conjugated donkey antimouse antibody (1:1,000, Invitrogen, USA). After washing and mounting in fluoro-gel aqueous medium, images were acquired on a fluorescent Olympus BX60 microscope equipped with an Olympus DP74 camera (Olympus, Spain). The numbers of cFos-labeled neurons in the central LC_{ipsi} and LC_{contra} were counted manually, represented as the mean + SD per LC slice, and each point corresponds to an individual animal. The numbers of cFos- and FG-labeled neurons in the central LC_{ipsi} and LC_{contra} were also counted manually using Fiji Image software (USA), expressed as the proportion of the total number of cFos-labeled neurons.

High-performance Liquid Chromatography

The noradrenaline (NA), dopamine (DA) and serotonin (5-HT) in the LC and rACC were evaluated, as were their metabolites 3,4-dihydroxyphenylacetic acid (DOPAC), homovanillic acid (HVA), and 5-hydroxyindoleacetic acid (5-HIAA). DA and DOPAC levels were also evaluated in the striatum as a control. All these compounds were analyzed by high-performance liquid chromatography (HPLC) on an apparatus equipped with a Elite Lachrom L-2130 pump (VWR, Hitachi, Japan) in conjunction with a glass carbon electrode set at −550 mV (DECADE II, ANTEC, The Netherlands). A Lichrocart cartridge (125 mm × 4 mm) column filled with Lichrospher reverse-phase C18 5-μm material (Merck, Germany) was used. The mobile phase consisted of a mixture of 0.05 M sodium acetate, 0.4 mM 1-octanesulfonic acid, 0.3 mM Na_2EDTA, and 70 ml methanol/l, adjusted to pH 4.1 with acetic acid. All reagents and water were HPLC-grade, and the flow rate was 1.0 ml/min. The measurement of all the molecules in fresh tissue was performed according to a method described previously.[33,34] The concentration (ng/g wet tissue) of NA, DA, 5-HT, DOPAC, HVA, and 5-HIAA was calculated with the aid of an eDAQPowerChrom 280 software (eDAQ, Australia) and represented as the mean ± SD.

Statistical Analysis

All the data were analyzed using STATISTICA 10.0 (StatSoft, USA) or GraphPad Prism 9 software (GraphPad Software, USA), and the results are all presented as the mean + SD, with each point corresponding to an individual animal. Statistical outliers were identified using Grubbs's test (GraphPad Software), and all the variables were tested for normality and homogeneity of variance using a Shapiro–Wilk test of normality. If the assumption of normality was unmet, a Kruskal–Wallis test followed by a Mann–Whitney U test was used. When all assumptions were met or when a nonparametric test cannot be carried out, unpaired *t* tests (two-tailed), or two-way, three-way, or repeated-measures ANOVA were performed, followed by the Tukey test to compare between more than two groups. In all cases, $P < 0.05$ was considered significant. The detailed statistical analysis is shown in Supplemental Digital Content 3 (Supplemental Statistical Tables 8 through 14, https://links.lww.com/ALN/D533).

Results

LC cFos Expression in the Short and Long Term after Neuropathy

The activity of LC neurons at two different time points after nerve injury (CCI-ST and CCI-LT), with (Stim[+]) or without (Stim[–]) noxious stimulation was explored by quantifying the cFos in these neurons (fig. 1). In the short term (fig. 1C), weak cFos expression was found in Stim(–) naive animals, which increased significantly and bilaterally in the LC after noxious hind paw stimulation (mean difference [95% CI], Stim[+] *vs.* Stim[–], LC_{ipsi}, –10.75 [95% CI, –18.96 to –2.54]%; ***$P < 0.001$; LC_{contra}, –9.25 [95% CI, –17.46 to –1.04]%; **$P < 0.01$). There was only modest cFos in unstimulated sham-ST animals, although this was significantly stronger in the LC_{ipsi} than in the LC_{contra} (mean difference [95% CI] relative to Stim[–], 6.83 [95% CI, –3.04 to 10.37]%; +$P < 0.05$) or in the LC_{ipsi} of naive animals (mean difference [95% CI] relative to Stim[–] LC_{ipsi}, –6.17 [95% CI, –13.66 to 1.33]%; #$P < 0.05$). This cFos expression was significantly enhanced on both sides of the LC by hind paw stimulation (mean difference [95% CI], Stim[+] *vs.* Stim[–], LC_{ipsi}, –10.83 [95% CI, –17.54 to –4.13]%; $P < 0.001$; LC_{contra}, –6.83 [95% CI, –13.54 to –0.13]%; **$P < 0.01$). Accordingly, cFos was expressed more strongly in the LC_{ipsi} of Stim(+) sham-ST animals than in the LC_{contra} (mean difference [95% CI], 7.67 [95% CI, 0.96 to 14.37]%; ++$P < 0.01$) or the LC_{ipsi} of naive animals (mean difference [95% CI], –6.25 [95% CI, –13.75 to 1.25]%; #$P < 0.05$). Hence, spontaneous cFos activity is lateralized in sham-ST animals, and it is enhanced by noxious stimulation. In the short term, the lateralized profile of cFos expression in nerve-injured animals without stimulation (Stim[–] CCI-ST) was similar to that in the sham-ST animals, albeit significantly stronger. As such, LC_{ipsi} expression was enhanced relative to the LC_{contra} in the former (mean difference [95% CI], 7.67 [95% CI, 0.96 to 14.37]%; +$P < 0.05$) and in the LC_{ipsi} of sham-ST animals (mean difference [95% CI], –11.33 [95% CI, –18.04 to –4.63]%; ###$P < 0.001$). After stimulation, cFos expression increased in the LC_{ipsi} relative to the Stim(–) CCI-ST (mean difference [95% CI], –9.67 [95% CI, –16.37 to –2.96]%; **$P < 0.01$), as well as to the Stim(+) LC_{contra} (mean difference [95% CI], 16.17 [95% CI, 9.46 to 22.87]%; +++$P < 0.001$) and the LC_{ipsi} of Stim(+) sham-ST animals (mean difference [95% CI], –10.17 [95% CI, –16.87 to –3.46]%; ###$P < 0.001$). In the CCI-ST LC_{contra}, cFos expression did not differ between Stim(+) and Stim(–) animals.

After long-term neuropathy, cFos expression was quantified in sham (sham-LT) and CCI (CCI-LT) animals (fig. 1D). The weak expression in the former was similar to that in naive animals, but it increased after noxious stimulation on both sides of the LC (mean difference [95% CI], Stim(+) *vs.* Stim(–), LC_{ipsi}, –16.33 [95% CI, –24.63 to –8.04]%; ***$P < 0.001$; LC_{contra}, –17.83 [–26.13 to –9.54]%; ***$P < 0.001$). There was a similar bilateral increase in cFos expression in the LC of CCI-LT animals relative to the Stim(–) sham-LT rats (mean difference [95% CI], LC_{ipsi}, –9.67 [95% CI, –17.96 to –1.37]%; ##$P < 0.01$; LC_{contra}, –12.50 [95% CI, –20.79 to –4.20]%; ###$P < 0.001$), and surprisingly, no change was produced by noxious stimulation of these CCI-LT animals.

We performed additional experiments in females in order to assess whether sex affected these results. When we replicated this experiment, we observed a similar LC cFos expression profile in both the female ST and LT rats after nerve injury (Supplemental Figure 6, Supplemental Digital Content 1, https://links.lww.com/ALN/D531).

cFos Expression by LC Neurons Projecting to the SC or rACC in the Short and Long Term after Neuropathy

To study the LC neurons projecting to the SC, the retrograde fluorescent FG tracer was administered to the ipsilateral superficial dorsal horn of the SC (fig. 2A). As expected, similar numbers of neurons were labeled in the LC_{ipsi} and LC_{contra} along the rostro-caudal axis (around 50%; fig. 2A), confirming the bilateral projection of the LC to the SC.[8] The activity of the LC→SC pathway was assessed by exploring cFos/FG colabeling in the short and long term after nerve injury in both Stim(+) and Stim(–) states (fig. 2, B through D). In the short term (fig. 2C), no cFos/FG positive neurons were found in either the LC_{ipsi} or LC_{contra} of Stim(–) sham-ST animals, whereas there was a significant number in the LC_{ipsi} (5.67 ± 3.50% cFos/FG + neurons relative to total cFos) than LC_{ipsi} of Stim(–) animals or LC_{contra} of Stim(+) animals (0.00 ± 0.00%, **,++$P < 0.01$). In CCI-ST animals, cFos expression increased in the Stim(–) LC_{ipsi} (3.83 ± 2.48%) relative to the LC_{contra} or the Stim(–) sham-ST animals (0.00 ± 0.00%; +,#$P < 0.05$). After stimulation, cFos expression increased in the LC_{ipsi} of CCI-ST animals (8.67 ± 3.98%) relative to the Stim(–) LC_{ipsi} (3.83 ± 2.48%; *$P < 0.05$) and Stim(+) LC_{contra} (0.00 ± 0.00%; +$P < 0.05$). Surprisingly, no c-Fos/FG-colabeled $LC_{ipsi/contra}$ neurons were detected in either sham-LT or CCI-LT rats, irrespective of stimulation (fig. 2D).

We previously demonstrated that the LC mainly projects unilaterally to the rACC (around 80%),[8] and as expected, bilateral administration of FG to the rACC labeled around 50% of the neurons in both sides of the LC (fig. 3A). We assessed the cFos/FG-labeled LC neurons projecting to the rACC in the short and long term after nerve injury (fig. 3, B through D). In the short term (fig. 3C), there was little cFos/FG colabeling in Stim(–) sham-ST animals, although this increased significantly after noxious stimulation in both the LC_{ipsi} (from 6.00 ± 1.58% to 38.40 ± 7.20%; $^{***}P < 0.001$) and LC_{contra} (from 6.80 ± 1.92% to 20.40 ± 4.56%; $^{**}P < 0.01$). Indeed, cFos expression in the LC_{ipsi} was induced more strongly by noxious stimulation than in the LC_{contra} ($++P < 0.01$). In Stim(–) CCI-ST animals, there were more cFos/FG-labeled LC_{ipsi} (42.80 ± 5.90%) and LC_{contra} (19.60 ± 3.65%) neurons relative to the total cFos neurons than in the respective sham-ST rats (LC_{ipsi} 6.00 ± 1.58%; $###P < 0.001$; and LC_{contra} 6.80 ± 1.92%; $##P < 0.01$). Notably, there were significantly more cFos/FG + neurons relative to the total cFos + neurons in the CCI-ST LC_{ipsi} than in the LC_{contra} ($+++P < 0.001$), a pattern that was not modified by noxious stimulation. In the long term (fig. 3D), no colabeling was found in Stim(–) sham-LT rats, yet there was a significant number of dual labeled cells after stimulation (Stim[+], LC_{ipsi} 41.17 ± 5.15%; $^{***}P < 0.001$; LC_{contra} 20.17 ± 4.67%; $^{**}P < 0.01$), with more dual labeled cells in the LC_{ipsi} than in the LC_{contra} ($+++P < 0.001$). In Stim(–) CCI-LT animals, a similar number of cFos/FG + neurons relative to the total cFos + neurons was found bilaterally in the LC (LC_{ipsi} 22.17 ± 3.60% and LC_{contra} 22.50 ± 3.33%), a pattern that was not modified by noxious stimulation.

Assessment of Spontaneous Pain-like Behaviors in Male and Female Neuropathic Rats

We performed experiments in female rats in order to evaluate whether sex influenced the spontaneous pain behavior of neuropathic rats, evaluating the spontaneous paw flinches in both male and female rats (Supplemental Figure 7, Supplemental Digital Content 1, https://links.lww.com/ALN/D531). As anticipated, animals performed more paw flinches after nerve injury relative to the sham animals in both the ST (mean difference [95% CI], –5.97 [95% CI, –7.69 to –4.25]%; $^{***}P < 0.001$) and LT (mean difference [95% CI], –18.25 [95% CI, –20.18 to –16.33]%; $^{***}P < 0.001$). However, it was notable that there were no discernible differences in the number of paw flinches between male and female rats at either of these time points.

Effect of Chemogenetic Modulation of Noradrenergic-LC Neurons in Spontaneous Pain-like Behaviors

To assess whether cFos expression correlates with spontaneous pain-like behaviors, the effect of chemogenetic manipulation of $LC_{ipsi/contra}$ activity was evaluated (fig. 4). Accordingly, selective hM4D(Gi)- or rM3D(Gs)-DREADD expression was induced in noradrenergic LC neurons of TH:Cre rats (Supplemental Figures 1 and 2, Supplemental Digital Content 1, https://links.lww.com/ALN/D531), as achieved previously,[28] and how hM4D(Gi)-DREADD–mediated LC inhibition affected the number of spontaneous paw flinches was assessed after systemic CNO administration (fig. 4B). As expected, nerve-injured animals produced significantly more paw flinches in both the ST (mean difference [95% CI] *vs.* sham-Sal, –4.20 [95% CI, –7.58 to –0.82]%; $^{*}P < 0.05$) and LT (mean difference [95% CI] *vs.* sham-Sal, –21.30 [95% CI, –25.14 to –17.46]%; $^{***}P < 0.001$). Moreover, while LC_{ipsi} blockade significantly increased the number of foot lifts in CCI-ST rats (mean difference [95% CI]. CCI-CNO *vs.* CCI-Sal, –5.50 [95% CI, –8.75 to –2.25]%; $++P < 0.01$), no such effect was evident in CCI-LT animals. By contrast, chemogenetically blocking the LC_{contra} had no significant effect in this spontaneous pain-like test at any time point postinjury.

Having previously demonstrated an increase in the mechanical and thermal pain thresholds after chemogenetic activation of LC_{ipsi} noradrenergic neurons in neuropathic TH:Cre Long–Evans rats,[8] we explored the effect of noradrenergic LC activation using rM3D(Gs)-DREADDs in CCI-LT animals (fig. 4C). CNO-mediated activation of the LC_{ipsi} significantly reduced the number of paw flinches relative to their controls (mean difference [95% CI], CCI-CNO *vs.* CCI-Sal, 18.63 [95% CI, 14.28 to 22.97]%; $+++P < 0.001$), whereas chemogenetic activation of LC_{contra} neurons did not significantly modify CCI-LT induced spontaneous pain-like behaviors. Finally, DREADD-mediated inactivation or activation of the noradrenergic $LC_{ipsi/contra}$ did not modify the number of paw flinches in any of the sham animals (fig. 4, B and C).

Effect of the Chemogenetic Modulation of the Noradrenergic LC→SC Pathway on Spontaneous Pain-like Behaviors

We explored how the noradrenergic-LC pathway descending to the SC influences the spontaneous pain-related phenotype using chemogenetics (fig. 5). As occurred after the global blockade of the LC (fig. 4B), DREADD-mediated inactivation of the noradrenergic LC_{ipsi}→SC pathway increased the number of paw flinches in CCI-ST rats (mean difference [95% CI], CCI-CNO *vs.* CCI-Sal, –5.00 [95% CI, –7.37 to –2.63]%; $+P < 0.05$), but not at later times. However, inhibition of the LC_{contra}→SC pathway produced no significant changes in this behavior (fig. 5A). Pathway activation by rM3D(Gs)-DREADD was also explored (fig. 5B), and like global LC_{ipsi} activation (fig. 4B), chemogenetic activation of the LC_{ipsi}→SC pathway dampened pain-related behaviors in CCI-ST (mean difference [95% CI], CCI-CNO *vs.* CCI-Sal, 5.08 [95% CI, 2.29 to 7.87]%; $++P < 0.01$) and CCI-LT rats (mean difference [95% CI], CCI-CNO *vs.* CCI-Sal, 10.67 [95% CI, 6.37 to 14.96]%; $+++P < 0.001$). Interestingly, activation of

the LC_{contra} neurons projecting to the SC also reduced the number of paw flinches by CCI-LT rats (mean difference [95% CI], CCI-CNO *vs.* CCI-Sal, 8.31 [95% CI, 4.73 to 11.89]%; +++$P < 0.001$). To verify whether the local activation of α2-adrenoreceptors in the SC produced analgesia in these animals, the α2-adrenoreceptor agonist clonidine was administered (20 μg/10 μl intrathecally), producing a clear analgesic effect in CCI-LT rats relative to those administered saline alone (mean difference [95% CI], 15.03 [95% CI, 11.62 to 18.45]%; ++$P < 0.01$; fig. 5C). Finally, global LC_{ipsi} or LC_{contra} activation or inhibition produced no change in the sham animals (fig. 5, A through C).

Effect of Chemogenetic Modulation of the Noradrenergic LC→rACC Pathway on Spontaneous Pain-like Behaviors and Pharmacologic Studies in the rACC

As one of the main ascending LC targets is the rACC, chemogenetic approaches were used to explore the role of these projections in spontaneous pain-like behavior (fig. 6). Chemogenetic blockade of the LC_{ipsi}→rACC but not the LC_{contra}→rACC pathway significantly decreased the number of paw flinches in CCI-ST animals relative to the CCI-Sal rats (mean difference [95% CI], 4.55 [95% CI, 0.73 to 8.30]%; +$P < 0.05$; fig. 6A). Moreover, and bearing in mind that the increase in cFos/FG expression was similar on both sides of the LC (fig. 3D), bilateral chemogenetic inhibition of this pathway significantly reduced the number of paw flinches in CCI-LT relative to the CCI-Sal rats (mean difference [95% CI], 17.02 [95% CI, 12.97 to 21.08]%; ++$P < 0.01$; fig. 6B).

Pharmacologic studies were then performed to explore the implication of adrenoreceptors on the rACC (fig. 7). Local administration of the α1-adrenoreceptor antagonist prazosin (5 μg/0.5 μl) reduced the number of paw flinches in CCI-ST animals relative to the saline controls (mean difference [95% CI], 3.12 [95% CI, 0.34 to 5.91]%; +$P < 0.05$), whereas the α2-adrenoreceptor antagonist idazoxan did not alter pain-like behavior (fig. 7A). Both Praz and Idx significantly reduced the number of paw flinches in the long term (mean difference [95% CI], CCI-Praz *vs.* CCI-Sal, 6.60 [95% CI, 2.43 to 10.77]%; +$P < 0.05$; CCI-Idx *vs.* CCI-Sal, 16.07 [95% CI, 9.94 to 22.20]%; +++$P < 0.001$; fig. 7B). As locomotor activity was not modified by any of these treatments (Supplemental Figures 3, 4, and 5, Supplemental Digital Content 1, https://links.lww.com/ALN/D531), these data suggest an involvement of α-adrenoreceptors in spontaneous pain-like behavior at the rACC level.

Levels of Monoamines and Their Metabolites in the LC and rACC

We previously showed that long-term neuropathy is associated with several plastic changes in the LC.[35,36] Hence, we explored whether nerve injury modifies the levels of NA, DA, and 5-HT, and of their metabolites DOPAC, HVA, and 5-HIAA, in the LC and rACC of CCI-ST and CCI-LT rats relative to the naive animals, using the striatum as a control tissue for DA and DOPAC levels. However, no differences in these compounds were detected between the distinct groups (see Supplemental Table 15, which contains the HPLC results, in Supplemental Digital Content 4, https://links.lww.com/ALN/D534).

Discussion

The data presented here reveal robust basal cFos activation in the LC_{ipsi}, both globally and in terms of its projections to the SC and rACC in CCI-ST animals. Chemogenetic approaches demonstrate that blocking the LC_{ipsi} or its projection to the SC enhances spontaneous pain-like behavior, whereas blocking its projection to the rACC reduces it. In long-term neuropathy, strong basal cFos expression is observed globally in the LC, particularly in the projection to the rACC, yet none is found in LC neurons projecting to the SC. Blocking the LC→rACC pathway with DREADDs reduces spontaneous pain-like behavior, whereas no effect is observed when blocking the LC globally or its projection to the SC. Thus, chemogenetic blockade of the LC globally or its projection to the SC yields similar results, while opposite actions are found when blocking the rACC at early and late stages of neuropathy. Moreover, no differences in the level of monoamines or their metabolites are found in the LC or rACC, suggesting that neuropathic pain does not induce global monoaminergic alterations, as occurs in other pathologies like multiple sclerosis,[37] Parkinson's,[38] or Alzheimer's disease.[39]

Immunohistochemistry reveals a significant basal increase in cFos expression in the LC_{ipsi} relative to the LC_{contra} in sham-ST rats, and a particularly robust increase in CCI-ST animals. A similar pattern of cFos expression is found in LC_{ipsi} neurons projecting to the SC, suggesting the side of the injury (*i.e.*, LC_{ipsi}) correlates with the level of damage, much higher in nerve-lesioned animals. This lateralized cFos expression is intriguing because brief nociceptive stimuli, such as that induced by mechanical stimulation or the injection of inflammatory mediators in the hind paw (carrageenan for 4 h), typically provokes bilateral LC cFos expression.[1,13] Hence, the duration of the insult (48 h) is probably responsible for sensitizing the LC_{ipsi}. This heightened cFos expression, especially in CCI-ST, may be involved in behaviors like anxiety[40–42] and arousal[43,44] but also in spontaneous pain. When exploring the latter, global chemogenetic blockade of the LC_{ipsi} or the specific projection to the SC significantly increases spontaneous pain-like behavior, whereas blocking the LC_{contra} provokes no change. These findings align with the fact that lesions, and pharmacologic or chemogenetic inactivation of the LC, exacerbate pain-evoked responses in several short-term pain states, indicating pain sensitivity is enhanced upon disruption of the normal LC-noradrenergic circuit.[8,24,45,46] This analgesic activity is mainly driven by the LC_{ipsi}, and it appears to be produced by activating the descending LC pathway to the

SC, which enhances noradrenaline release and in turn contributes to the blockade of ascending nociceptive inputs.[6,8,16]

Another relevant pathway is that of the LC→rACC, as lesion[47,48] or injection of a brain-derived neurotrophic factor (BDNF)–tropomyosin receptor kinase B (TrkB) antagonist into the rACC completely blocks the conditioned place preference induced by the α-2 adrenoreceptor agonist Cloni.[48,49] Hence, the ACC appears to be necessary to regulate spontaneous pain. In CCI-ST animals, there is also a strong and lateralized activity in this region, such that chemogenetic blockade of the LC_{ipsi}→rACC dampens spontaneous pain, yet no effect is found when the LC_{contra} is manipulated. Overall, this suggests that lateralized cFos expression is related to spontaneous pain-like behavior, albeit in opposing directions depending on the projection.

In long-term neuropathy, lateralized cFos expression is lost, and while strong expression is found in the LC globally,[8,50] this is not the case for cells projecting to the SC. DREADDs-mediated blockade of either the LC_{ipsi} or the LC_{contra} globally or of the specific projection to the SC does not modify spontaneous pain-like behaviors. This response is consistent with the belief that the LC does not induce endogenous analgesia through the descending projection to the SC when neuropathy becomes long-term.[8,51] There is also a robust bilateral increase in cFos at the ACC level in CCI-LT, and there is a reduction in spontaneous pain-like behaviors when the $LC_{ipsi/contra}$ is blocked. Hence, the LC→rACC projection appears to fulfill a pronociceptive role in both short- and long-term pain. This aligns with previous findings showing that chemogenetic activation of the LC→Prefrontal cortex projection exacerbates spontaneous pain, produces aversion, and increases anxiety-like behavior in neuropathic pain animals.[16] On the other hand, when the LC is chemogenetically activated globally, or simply its projection to the SC, there is significant relief of pain-related behaviors.[8] These chemogenetic studies are consistent with the pharmacologic effects of the acute intrathecal administration of the selective noradrenergic reuptake inhibitor reboxetine, which relieves evoked pain and induces conditioned place preference. However, acute systemic reboxetine administration also relieves evoked pain, although it is aversive in the conditioned place preference paradigm.[52] Hence, the beneficial effect of noradrenaline at the SC is probably counteracted by the activation of other supraspinal noradrenergic projections.

Our data also suggest that the hyperactivity of the LC→rACC projection that induces spontaneous pain-like behavior is mediated by activation of α-1 adrenoreceptors over the short term, and by α-1 and α-2 adrenoreceptors in the long term. Previous findings showed microinjection of the α-2 adrenoreceptors agonist Cloni into the ACC alleviates spontaneous pain-like behavior at day 7 but not at 14 days after nerve injury in common peroneal nerve–ligated mice.[48] These data, in a different animal model, suggest an analgesic effect of ACC α-2 adrenoreceptor activation, which contrasts with our findings, although it is consistent with the dynamic regulation of cingulate α-adrenoreceptors over time after nerve injury.

We also explored cFos levels after mechanical noxious stimulation of a hind paw. In naive animals, cFos was only weakly expressed, but it increased bilaterally and uniformly in the LC when noxious stimulation was applied to one hind paw, consistent with previous data.[11,13] Sham animals behave like naive animals in the long term, which may indicate satisfactory resolution of the damage produced by the sham intervention. Findings from naive and sham-LT animals suggest that bilateral activation of the LC during acute unilateral hind paw pain could partly reflect the modulation of nociceptive processing in the SC dorsal horn. However, this is unlikely because this pathway is not endogenously activated when FG/cFos colabeling of neurons is explored in sham-LT animals. Furthermore, chemogenetic inhibition of LC-noradrenergic neurons or intra-LC lidocaine administration did not modify sensorial responses in sham-LT animals.[2,8,24,53] Another possibility is that this bilateral LC activation is related to other nonsensorial aspects of pain, such as the inherent stress associated with the pain experience itself.[7,54] In this sense, restraint stress increases anxiety behavior and cFos immunoreactivity in LC neurons, and the chemogenetic inhibition of LC-noradrenergic neurons prevents stress-induced anxiety.[40] Therefore, LC activity appears to have a minor influence on evoked hypersensitivity in these conditions, which could be related to a stress-related response.

In sham-ST animals, the lateralized basal cFos expression is further enhanced by noxious stimulation of the hind paw. Interestingly, similar data were obtained from the LC_{ipsi} of CCI-ST rats, although cFos expression was significantly stronger, suggesting that the LC responses at this point of neuropathy resemble other forms of short-term injury, yet they are more intense. Furthermore, cFos expression in the CCI-ST LC_{contra} did not differ significantly from that in the LC_{contra} of sham animals, and it did not change upon noxious stimulation, perhaps suggesting that the LC_{contra} had already reached its maximum possible response. These data are consistent with the significant increase in hypersensitivity to a cold stimulus in CCI-ST animals after chemogenetic inhibition of the LC_{ipsi}.[8] Furthermore, we previously found that pharmacologic blockade with lidocaine significantly increased the nociceptive threshold of Sprague–Dawley rats.[24] As no effect was found when blocking the LC_{contra},[8,24] endogenous LC-driven analgesia in the short term under evoked conditions appears to be mediated through the LC_{ipsi}.

A very different profile is found in the long term after neuropathy, whereby the baseline increase in cFos expression is not altered by noxious stimuli, either globally in the LC or in the specific projections to the SC or rACC. This is consistent with earlier data showing that 11 days of nerve injury attenuated restraint-induced global LC cFos expression,[55] suggesting that long-term nerve injury might

impair the ordinary cellular response of the LC to an acute stimulus. This is again in line with reduced LC-mediated descending inhibitory controls or diminished analgesic efficacy of drugs targeting LC pathways described previously.[56–60] Accordingly, chemogenetic blockade of the LC_{ipsi} or LC_{contra} at CCI-LT does not modify the response to acetone,[8] suggesting that this increase in cFos is not related to the sensory dimension of pain. However, blockade of the LC_{contra} with lidocaine elevates the nociceptive threshold in CCI-LT Sprague–Dawley rats.[24] Furthermore, enhanced LC electrophysiologic responses are produced by mechanical stimulation of the nerve-injured paw at CCI-LT, predominantly mediated by the LC_{contra}.[61] These findings align with the responses of Sprague–Dawley rats to bilateral microinjections of lidocaine into the LC, which completely reverse the behavioral signs of neuropathy 2 weeks after nerve injury.[62] Overall, the LC seems to fulfill distinct roles depending on the rat strain, with a lateralized pronociceptive activity of the LC associated with long-term neuropathy in Sprague–Dawley but not Long–Evans rats. These discrepancies may reflect the reported strain differences in the noradrenergic pathways of these animals.[63–66]

The new data presented here suggest that bilateral LC or LC→SC projections fulfill an analgesic role in spontaneous and evoked conditions, mainly due to the activation of the LC_{ipsi}, although activation of the LC_{ipsi}→rACC pathway partially counteracts endogenous analgesia in response to spontaneous pain. In the long term, cFos is expressed strongly on a global level in response to pain, and in the rACC, yet it is no longer lateralized and there is no activation in the SC. Importantly, cFos expression is not modified by nociceptive stimulation after long-term pain. At this time point, the analgesic contribution of the LC is lost, and the activity of the LC_{ipsi}→rACC pathway in promoting spontaneous pain predominates. Anticipating forthcoming electrophysiologic studies to complement these experiments, specific LC projections to the SC or rACC appear to have different behavioral effects depending on the time that has passed since the injury. Moreover, other projection areas like the dorsal reticular nucleus[24] or insular cortex[67] could also potentially contribute to the spontaneous pain mediated by the LC and warrant further exploration. Future studies utilizing the targeted recombination of active populations (TRAP) approach[68–70] could provide insights as to whether distinct subpopulations within the LC are recruited for spontaneous pain, and help elucidate their physiologic and molecular characteristics. Finally, although our study did not reveal differences between male and female rats, it is crucial to include both sexes in such research to comprehensively understand any sexual dimorphism or common behaviors related to these phenomena.

Acknowledgments

The authors are very grateful to Jose Antonio Garcia Partida, M.Sc., University of Cádiz (Cádiz, Spain), and Elena Marín Álvarez, Higher Technician, University of Cádiz (Cádiz, Spain) for their excellent technical assistance. They also acknowledge the assistance of the Central Services of Scientific and Technological Research, Health Sciences and Animal Research at the University of Cádiz.

Research Support

This study was supported by grants PID2022-142785OB-I00 and PDC2022-133987-100 funded by MCIN/AEI/10.13039/501100011033 and, as appropriate, by "ERDF A way of making Europe," by the European Union and European Union NextGenerationEU/PRTR respectively, by Andalusian Regional Ministry of Health (Spain) (PI-0134-2018; No. P20-00958), by the Regional Operational Program for Andalucía FEDER, by the Biomedical Research and Innovation Institute of Cádiz (INIBICA, Spain) (IN-C09), by the Andalusian Regional Ministry of Economy, Innovation, Science and Employment (Spain) (CTS-510), and by the Biomedical Research Networking Center for Mental Health (CIBERSAM, Spain) (CB07/09/0033). The figures were generated with BioRender.com (BioRender, Canada).

Competing Interests

The authors declare no competing interests.

Correspondence

Address correspondence to Dr. Berrocoso: Neuropsychopharmacology and Psychobiology Research Group, Department of Neuroscience, Faculty of Medicine, University of Cádiz, 11003 Cádiz, Spain. esther.berrocoso@uca.es

Supplemental Digital Content

Supplemental Digital Content 1: Supplemental Figures, https://links.lww.com/ALN/D531
Supplemental Digital Content 2: Sample Size Tables 1 through 7, https://links.lww.com/ALN/D532
Supplemental Digital Content 3: Statistical Tables 8 through 14, https://links.lww.com/ALN/D533
Supplemental Digital Content 4: Table 15: HPLC Results, https://links.lww.com/ALN/D534

References

1. Llorca-Torralba M, Borges G, Neto F, Mico JA, Berrocoso E: Noradrenergic locus coeruleus pathways in pain modulation. Neuroscience 2016; 338:93–113
2. Schwarz LA, Luo L: Organization of the locus coeruleus-norepinephrine system. Curr Biol 2015; 25:R1051–6

3. Poe GR, Foote S, Eschenko O, et al.: Locus coeruleus: A new look at the blue spot. Nat Rev Neurosci 2020; 21:644–59
4. Jones SL, Gebhart GF: Quantitative characterization of ceruleospinal inhibition of nociceptive transmission in the rat. J Neurophysiol 1986; 56:1397–410
5. Jasmin L, Boudah A, Ohara PT: Long-term effects of decreased noradrenergic central nervous system innervation on pain behavior and opioid antinociception. J Comp Neurol 2003; 460:38–55
6. Tsuruoka M, Matsutani K, Inoue T: Coeruleospinal inhibition of nociceptive processing in the dorsal horn during unilateral hindpaw inflammation in the rat. Pain 2003; 104:353–61
7. Suárez-Pereira I, Llorca-Torralba M, Bravo L, Camarena-Delgado C, Soriano-Mas C, Berrocoso E: The role of the locus coeruleus in pain and associated stress-related disorders. Biol Psychiatry 2022; 91:786–97
8. Llorca-Torralba M, Camarena-Delgado C, Suárez-Pereira I, et al.: Pain and depression comorbidity causes asymmetric plasticity in the locus coeruleus neurons. Brain 2022; 145:154–67
9. Nestler EJ, Barrot M, Self DW: DeltaFosB: A sustained molecular switch for addiction. Proc Natl Acad Sci U S A 2001; 98:11042–6
10. Hebert MA, Serova LI, Sabban EL: Single and repeated immobilization stress differentially trigger induction and phosphorylation of several transcription factors and mitogen-activated protein kinases in the rat locus coeruleus. J Neurochem 2005; 95:484–98
11. Voisin DL, Guy N, Chalus M, Dallel R: Nociceptive stimulation activates locus coeruleus neurones projecting to the somatosensory thalamus in the rat. J Physiol 2005; 566:929–37
12. Baulmann J, Spitznagel H, Herdegen T, Unger T, Culman J: Tachykinin receptor inhibition and c-Fos expression in the rat brain following formalin-induced pain. Neuroscience 2000; 95:813–20
13. Tsuruoka M, Arai YC, Nomura H, Matsutani K, Willis WD: Unilateral hindpaw inflammation induces bilateral activation of the locus coeruleus and the nucleus subcoeruleus in the rat. Brain Res Bull 2003; 61:117–23
14. Finnerup NB, Kuner R, Jensen TS: Neuropathic pain: From mechanisms to treatment. Physiol Rev 2021; 101:259–301
15. Chandler DJ, Jensen P, McCall JG, Pickering AE, Schwarz LA, Totah NK: Redefining noradrenergic neuromodulation of behavior: Impacts of a modular locus coeruleus architecture. J Neurosci 2019; 39:8239–49
16. Hirschberg S, Li Y, Randall A, Kremer EJ, Pickering AE: Functional dichotomy in spinal- vs prefrontal-projecting locus coeruleus modules splits descending noradrenergic analgesia from ascending aversion and anxiety in rats. Elife 2017; 6:e29808
17. Singh A, Patel D, Li A, et al.: Mapping cortical integration of sensory and affective pain pathways. Curr Biol 2020; 30:1703–15.e5
18. Sellmeijer J, Mathis V, Hugel S, et al.: Hyperactivity of anterior cingulate cortex areas 24a/24b drives chronic pain-induced anxiodepressive-like consequences. J Neurosci 2018; 38:3102–15
19. Kilkenny C, Browne WJ, Cuthill IC, Emerson M, Altman DG: Improving bioscience research reporting: The ARRIVE guidelines for reporting animal research. PLoS Biol 2010; 8:e1000412
20. Bennett GJ, Xie YK: A peripheral mononeuropathy in rat that produces disorders of pain sensation like those seen in man. Pain 1988; 33:87–107
21. Berrocoso E, De Benito MD, Mico JA: Role of serotonin 5-HT1A and opioid receptors in the antiallodynic effect of tramadol in the chronic constriction injury model of neuropathic pain in rats. Psychopharmacology (Berl) 2007; 193:97–105
22. Cora MC, Kooistra L, Travlos G: Vaginal cytology of the laboratory rat and mouse: Review and criteria for the staging of the estrous cycle using stained vaginal smears. Toxicol Pathol 2015; 43:776–93
23. Faul F, Erdfelder E, Lang AG, Buchner A: G*Power 3: A flexible statistical power analysis program for the social, behavioral, and biomedical sciences. Behav Res Methods 2007; 39:175–91
24. Camarena-Delgado C, Llorca-Torralba M, Suárez-Pereira I, et al.: Nerve injury induces transient locus coeruleus activation over time: role of the locus coeruleus-dorsal reticular nucleus pathway. Pain 2022; 163:943–54
25. Paxinos G, Watson C: The Rat Brain in Stereotaxic Coordinates. 6th ed., San Diego. Elsevier Academic Press, 2007.
26. Takeda R, Watanabe Y, Ikeda T, et al.: Analgesic effect of milnacipran is associated with c-Fos expression in the anterior cingulate cortex in the rat neuropathic pain model. Neurosci Res 2009; 64:380–4
27. Alba-Delgado C, Mico JA, Sánchez-Blázquez P, Berrocoso E: Analgesic antidepressants promote the responsiveness of locus coeruleus neurons to noxious stimulation: Implications for neuropathic pain. Pain 2012; 153:1438–49
28. Llorca-Torralba M, Suárez-Pereira I, Bravo L, et al.: Chemogenetic silencing of the locus coeruleus-basolateral amygdala pathway abolishes pain-induced anxiety and enhanced aversive learning in rats. Biol Psychiatry 2019; 85:1021–35
29. Bravo L, Alba-Delgado C, Torres-Sanchez S, Mico JA, Neto FL, Berrocoso E: Social stress exacerbates the aversion to painful experiences in rats exposed to chronic pain: The role of the locus coeruleus. Pain 2013; 154:2014–23

30. Wei H, Viisanen H, You HJ, Pertovaara A: Spinal histamine in attenuation of mechanical hypersensitivity in the spinal nerve ligation-induced model of experimental neuropathy. Eur J Pharmacol 2016; 772:1–10
31. Mahler SV, Aston-Jones G: CNO evil? Considerations for the use of DREADDs in behavioral neuroscience. Neuropsychopharmacology 2018; 43:934–6
32. Goutaudier R, Coizet V, Carcenac C, Carnicella S: DREADDs: the power of the lock, the weakness of the key. Favoring the pursuit of specific conditions rather than specific ligands. eNeuro 2019; 6:ENEURO.0171-19.2019
33. Gallardo E, Madrona A, Palma-Valdes R, Espartero JL, Santiago M: Effect of intracerebral hydroxytyrosol and its nitroderivatives on striatal dopamine metabolism: A study by in vivo microdialysis. Life Sci 2015; 134:30–5
34. Suárez-Pereira I, García-Domínguez I, Bravo L, et al.: The absence of caspase-8 in the dopaminergic system leads to mild autism-like behavior. Front Cell Dev Biol 2022; 10:839715
35. Bravo L, Mariscal P, Llorca-Torralba M, López-Cepero JM, Nacher J, Berrocoso E: Altered expression of vesicular glutamate transporter-2 and cleaved caspase-3 in the locus coeruleus of nerve-injured rats. Front Mol Neurosci 2022; 15:918321
36. Alba-Delgado C, Llorca-Torralba M, Horrillo I, et al.: Chronic pain leads to concomitant noradrenergic impairment and mood disorders. Biol Psychiatry 2013; 73:54–62
37. Polak PE, Kalinin S, Feinstein DL: Locus coeruleus damage and noradrenaline reductions in multiple sclerosis and experimental autoimmune encephalomyelitis. Brain 2011; 134:665–77
38. Pavese N, Rivero-Bosch M, Lewis SJ, Whone AL, Brooks DJ: Progression of monoaminergic dysfunction in Parkinson's disease: A longitudinal 18F-dopa PET study. Neuroimage 2011; 56:1463–8
39. Šimić G, Leko MB, Wray S, et al.: Monoaminergic neuropathology in Alzheimer's disease. Prog Neurobiol 2017; 151:101–38
40. McCall JG, Al-Hasani R, Siuda ER, et al.: CRH engagement of the locus coeruleus noradrenergic system mediates stress-induced anxiety. Neuron 2015; 87:605–20
41. Morris LS, McCall JG, Charney DS, Murrough JW: The role of the locus coeruleus in the generation of pathological anxiety. Brain Neurosci Adv 2020; 4:2398212820930321
42. Borodovitsyna O, Duffy BC, Pickering AE, Chandler DJ: Anatomically and functionally distinct locus coeruleus efferents mediate opposing effects on anxiety-like behavior. Neurobiol Stress 2020; 13:100284
43. Hagan JJ, Leslie RA, Patel S, et al.: Orexin A activates locus coeruleus cell firing and increases arousal in the rat. Proc Natl Acad Sci U S A 1999; 96:10911–6
44. Breton-Provencher V, Sur M: Active control of arousal by a locus coeruleus GABAergic circuit. Nat Neurosci 2019; 22:218–28
45. Bodnar RJ, Ackermann RF, Kelly DD, Glusman M: Elevations in nociceptive thresholds following locus coeruleus lesions. Brain Res Bull 1978; 3:125–30
46. Martin WJ, Gupta NK, Loo CM, Rohde DS, Basbaum AI: Differential effects of neurotoxic destruction of descending noradrenergic pathways on acute and persistent nociceptive processing. Pain 1999; 80:57–65
47. Qu C, King T, Okun A, Lai J, Fields HL, Porreca F: Lesion of the rostral anterior cingulate cortex eliminates the aversiveness of spontaneous neuropathic pain following partial or complete axotomy. Pain 2011; 152:1641–8
48. Wang YJ, Zuo ZX, Wu C, Liu L, Feng ZH, Li XY: Cingulate alpha-2A adrenoceptors mediate the effects of clonidine on spontaneous pain induced by peripheral nerve injury. Front Mol Neurosci 2017; 10:289
49. Zhang L, Wang G, Ma J, et al.: Brain-derived neurotrophic factor (BDNF) in the rostral anterior cingulate cortex (rACC) contributes to neuropathic spontaneous pain-related aversion via NR2B receptors. Brain Res Bull 2016; 127:56–65
50. Llorca-Torralba M, Pilar-Cuéllar F, Bravo L, et al.: Opioid activity in the locus coeruleus is modulated by chronic neuropathic pain. Mol Neurobiol 2019; 56:4135–50
51. Hughes SW, Hickey L, Hulse RP, Lumb BM, Pickering AE: Endogenous analgesic action of the pontospinal noradrenergic system spatially restricts and temporally delays the progression of neuropathic pain following tibial nerve injury. Pain 2013; 154:1680–90
52. Hughes S, Hickey L, Donaldson LF, Lumb BM, Pickering AE: Intrathecal reboxetine suppresses evoked and ongoing neuropathic pain behaviours by restoring spinal noradrenergic inhibitory tone. Pain 2015; 156:328–34
53. Safari MS, Haghparast A, Semnanian S: Effect of lidocaine administration at the nucleus locus coeruleus level on lateral hypothalamus-induced antinociception in the rat. Pharmacol Biochem Behav 2009; 92:629–34
54. Ross JA, Van Bockstaele EJ: The locus coeruleus-norepinephrine system in stress and arousal: Unraveling historical, current, and future perspectives. Front Psychiatry 2020; 11:601519
55. Boorman DC, Kang JWM, Keay KA: Peripheral nerve injury attenuates stress-induced Fos-family expression in the locus coeruleus of male Sprague-Dawley rats. Brain Res 2019; 1719:253–62
56. Kimura M, Suto T, Morado-Urbina CE, Peters CM, Eisenach JC, Hayashida KI: Impaired pain-evoked

analgesia after nerve injury in rats reflects altered glutamate regulation in the locus coeruleus. Anesthesiology 2015; 123:899–908
57. Kimura M, Eisenach JC, Hayashida KI: Gabapentin loses efficacy over time after nerve injury in rats: Role of glutamate transporter-1 in the locus coeruleus. Pain 2016; 157:2024–32
58. Kato D, Suto T, Obata H, Saito S: Spinal activation of tropomyosin receptor kinase-B recovers the impaired endogenous analgesia in neuropathic pain rats. Anesth Analg 2019; 129:578–86
59. Patel R, Qu C, Xie JY, Porreca F, Dickenson AH: Selective deficiencies in descending inhibitory modulation in neuropathic rats: Implications for enhancing noradrenergic tone. Pain 2018; 159:1887–99
60. Matsuoka H, Suto T, Saito S, Obata H: Amitriptyline, but not pregabalin, reverses the attenuation of noxious stimulus–induced analgesia after nerve injury in rats. Anesth Analg 2019; 123:504–10
61. Alba-Delgado C, Mico JA, Berrocoso E: Neuropathic pain increases spontaneous and noxious-evoked activity of locus coeruleus neurons. Prog Neuropsychopharmacol Biol Psychiatry 2021; 105:110121
62. Brightwell JJ, Taylor BK: Noradrenergic neurons in the locus coeruleus contribute to neuropathic pain. Neuroscience 2009; 160:174–85
63. Mogil JS: Animal models of pain: progress and challenges. Nat Rev Neurosci 2009; 10:283–94
64. Clark FM, Yeomans DC, Proudfit HK: The noradrenergic innervation of the spinal cord: Differences between two substrains of Sprague-Dawley rats determined using retrograde tracers combined with immunocytochemistry. Neurosci Lett 1991; 125:155–8
65. Sluka KA, Westlund KN: Spinal projections of the locus coeruleus and the nucleus subcoeruleus in the Harlan and the Sasco Sprague-Dawley rat. Brain Res 1992; 579:67–73
66. De Felice M, Sanoja R, Wang R, et al.: Engagement of descending inhibition from the rostral ventromedial medulla protects against chronic neuropathic pain. Pain 2011; 152:2701–9
67. Labrakakis C: The role of the insular cortex in pain. Int J Mol Sci 2023; 24:5736
68. DeNardo LA, Liu CD, Allen WE, et al.: Temporal evolution of cortical ensembles promoting remote memory retrieval. Nat Neurosci 2019; 22:460–9
69. Xing B, Mack NR, Guo KM, et al.: A subpopulation of prefrontal cortical neurons is required for social memory. Biol Psychiatry 2021; 89:521–31
70. Guenthner CJ, Miyamichi K, Yang HH, Heller HC, Luo L: Permanent genetic access to transiently active neurons via TRAP: Targeted recombination in active populations. Neuron 2013; 78:773–84